

Re: yesterday

The nature of mean-field generation in three classes of optimal dynamos

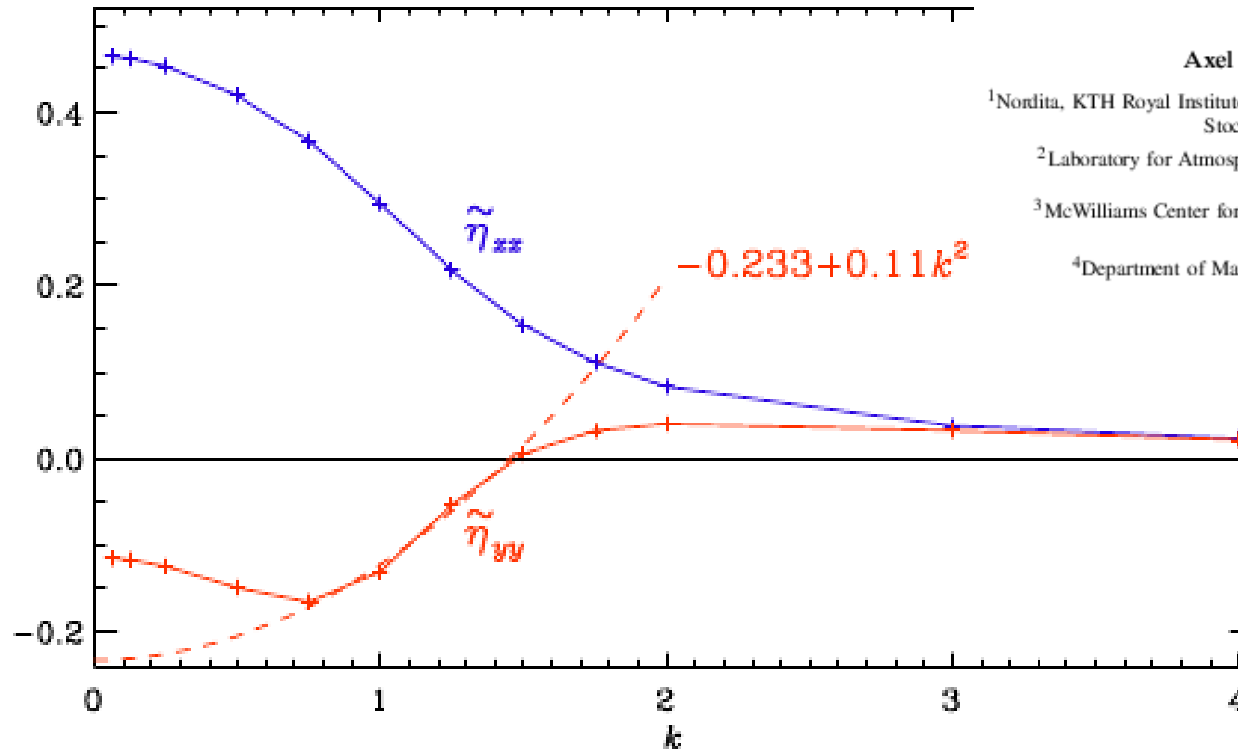
Axel Brandenburg^{1,2,3,†} and Long Chen⁴

¹Nordita, KTH Royal Institute of Technology and Stockholm University, and Department of Astronomy, Stockholm University, SE-10691 Stockholm, Sweden

²Laboratory for Atmospheric and Space Physics and JILA, University of Colorado, Boulder, CO 80303, USA

³McWilliams Center for Cosmology and Department of Physics, Carnegie Mellon University, Pittsburgh, PA 15213, USA

⁴Department of Mathematical Sciences, Durham University, Durham DH1 3LE, UK



Negative diffusivity, but
positive hyperdiffusivity
(positive curvature!)

$$\frac{\partial \bar{A}_y}{\partial t} = [\eta + \tilde{\eta}_{yy}^{(0)}] \frac{\partial^2 \bar{A}_y}{\partial z^2} - \tilde{\eta}_{yy}^{(2)} \frac{\partial^4 \bar{A}_y}{\partial z^4}.$$

We thank the anonymous reviewers and P. Livermore for their useful comments and M. Käpylä, A. Pevtsov, I. Virtanen and N. Yokoi for providing a splendid atmosphere at the Nordita-supported program on Solar Helicities in Theory and Observations.

Preprint numbers

THE ASTROPHYSICAL JOURNAL, 625:539–547, 2005 May 20

© 2005. The American Astronomical Society. All rights reserved. Printed in U.S.A.

Comments: 10 pages, 6 figures, *Astrophys. J.* 625
Subjects: **Astrophysics (astro-ph)**
Journal reference: *Astrophys.J.* 625 (2005) 539-547
DOI: [10.1086/429584](https://doi.org/10.1086/429584)
Report number: NORDITA-2005-15
Cite as: [arXiv:astro-ph/0502275](https://arxiv.org/abs/astro-ph/0502275)

THE CASE FOR A DISTRIBUTED SOLAR DYNAMO SHAPED BY NEAR-SURFACE SHEAR

AXEL BRANDENBURG

Isaac Newton Institute for Mathematical Sciences, 20 Clarkson Road, Cambridge CB3 0EH, UK;
and Nordita, Blegdamsvej 17, DK-2100 Copenhagen Ø, Denmark; brandenb@nordita.dk

Received 2004 December 15; accepted 2005 February 10

THE ASTROPHYSICAL JOURNAL, 550:824–840, 2001 April 1

© 2001. The American Astronomical Society. All rights reserved. Printed in U.S.A.

Comments: 21 pages, 26 figures, *ApJ* (accepted)
Subjects: **Astrophysics (astro-ph)**
Journal reference: *Astrophys.J.* 550:824-840, 2001
DOI: [10.1086/319783](https://doi.org/10.1086/319783)
Report number: NORDITA 2000/57 AP and NSF-ITP-00-55
Cite as: [arXiv:astro-ph/0006186](https://arxiv.org/abs/astro-ph/0006186)

THE INVERSE CASCADE AND NONLINEAR ALPHA-EFFECT IN SIMULATIONS OF ISOTROPIC HELICAL HYDROMAGNETIC TURBULENCE

AXEL BRANDENBURG^{1,2}

Institute for Theoretical Physics, Kohn Hall, University of California, Santa Barbara, Santa Barbara, CA 93106; brandenb@nordita.dk

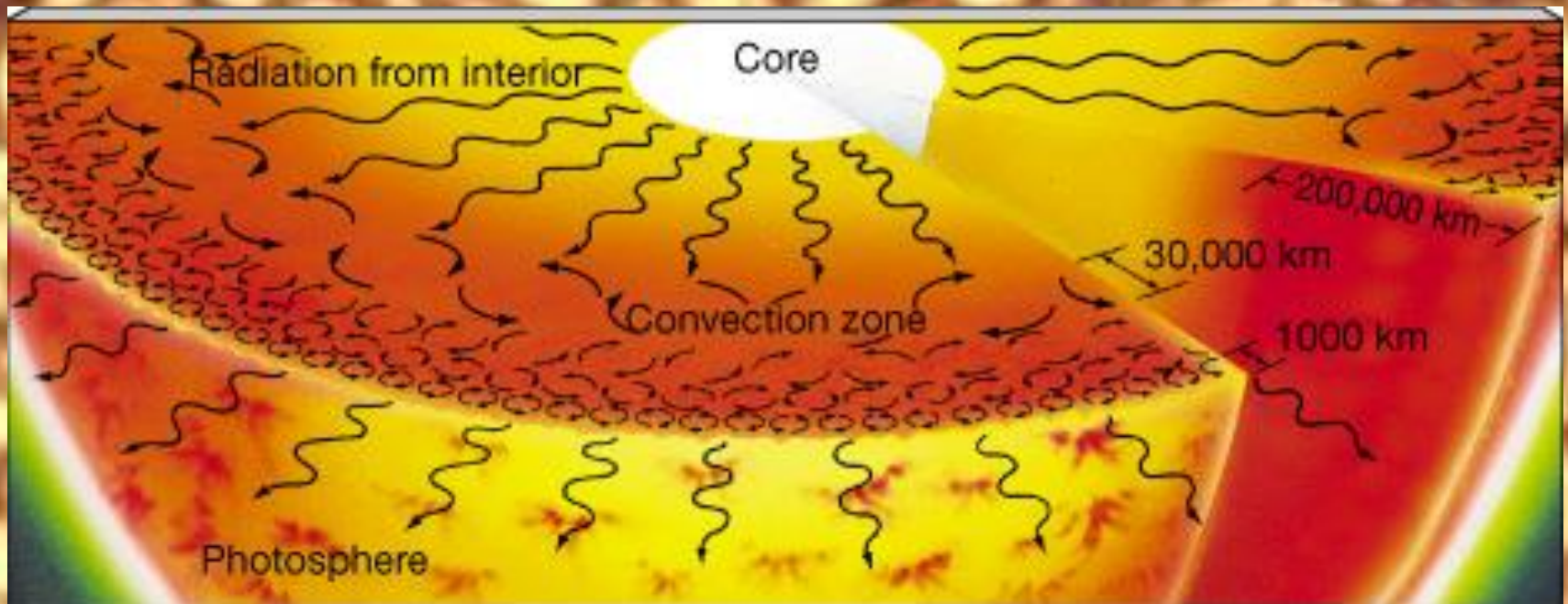
Received 2000 June 12; accepted 2000 December 8

Entropy Rain

Surface: granulation ($\sim 1\text{Mm}$)

Radius of the Sun: 700 Mm

Convection zone: 200 Mm



Early work in the 1930s

Sternwarte Berlin-Babelsberg, 1937 Nov. 20.

L. Biermann.

Zur Theorie der Granulation und der Wasserstoffkonvektionszone der Sonne.

Von *L. Biermann.*

Als Dicke der WKZ findet Siedentopf 700 km für den von *Unsöld* angenommenen Wasserstoffgehalt (27⁰/₀), und als Durchmesser der Granula nimmt er 500 km an. Die beobach-

On the Convection of the Stellar Photospheres*

Sueo UENO and Satoshi MATSUSHIMA

Institute of Astrophysics, Kyoto University

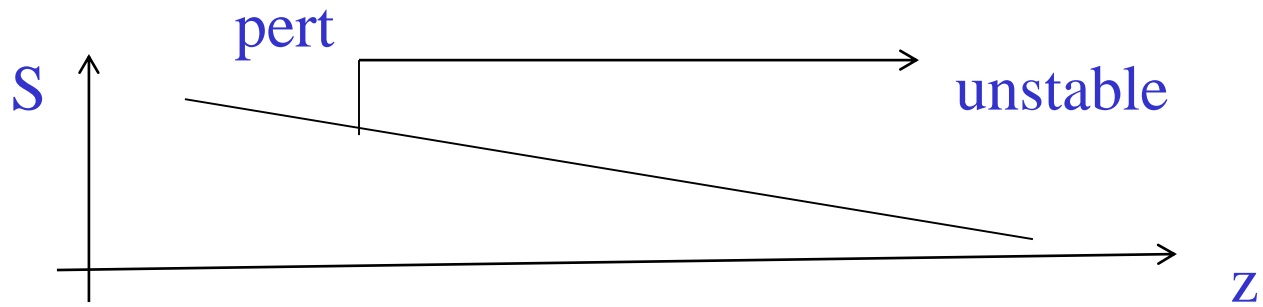
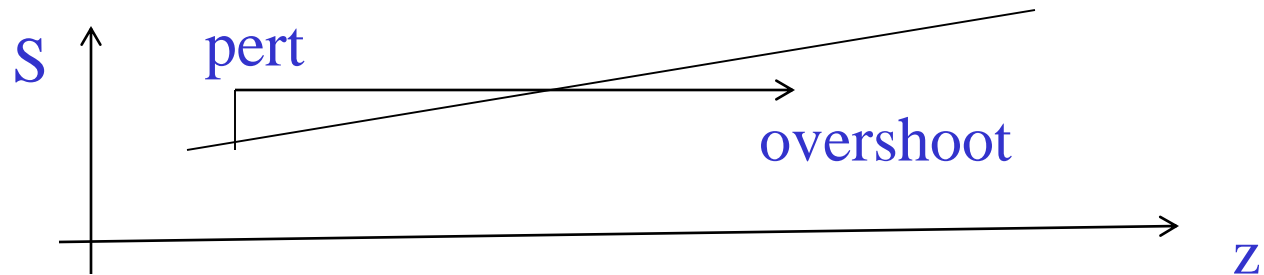
(Received May 4, 1950)

In these earlier works, the opacity of the stellar photospheres has been attributed to the continuous absorption of neutral hydrogen for the early type stars and to that of various metallic atoms for the late type stars. But, since 1938 it has been pointed out by R. Wildt⁽⁶⁾ that for the late type stars the opacity of negative hydrogen ion instead of metals plays a leading role in the mechanism of continuous absorption, the effect on the photospheric structure has become to be considered as relevant, as has been shown by R. Wildt⁽⁷⁾ and B. Strömgren⁽⁸⁾. Several years later, the coefficient of continuous absorptions of H⁻ has been in detail computed by Chandrasekhar and his collaborators⁽⁹⁾. Consequently it may be of interest to revise the theory of convection allowing for the continuous absorptions of atoms and negative ions of hydrogen.

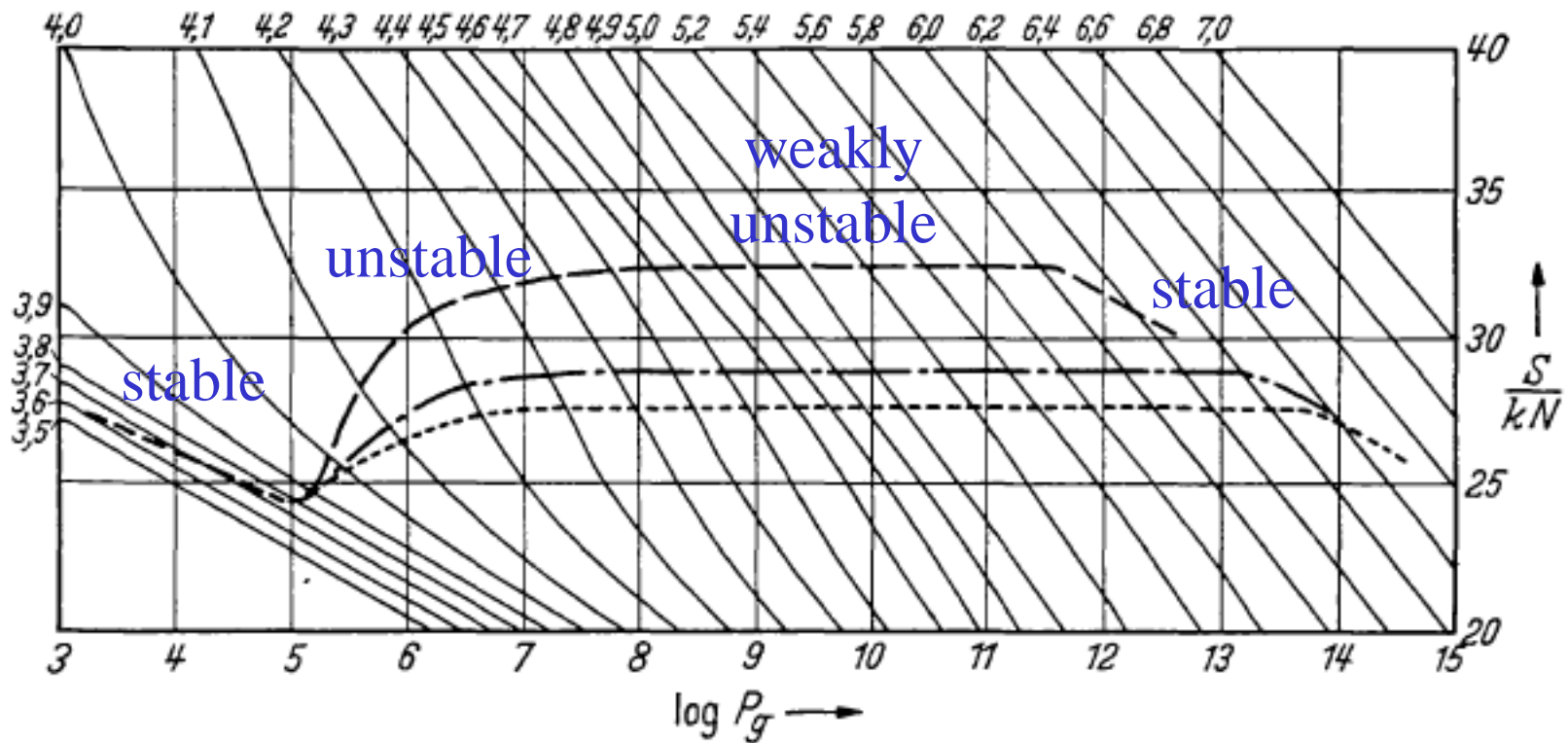
Entropy & convection

$$S / c_p = \frac{1}{\gamma} \ln p - \ln \rho$$

Adiabatic changes: $S = \text{const}$
P equilibrium: $S+ \rightarrow$ buoyant



Original mixing length model



surface

Von

interior

ERIKA VITENSE, Kiel.

Mit 11 Textabbildungen.

(Eingegangen am 15. November 1952.)

Anomalous weak solar convection

Shravan M. Hanasoge^{a,b,1}, Thomas L. Duvall, Jr.^c, and Katepalli R. Sreenivasan^d

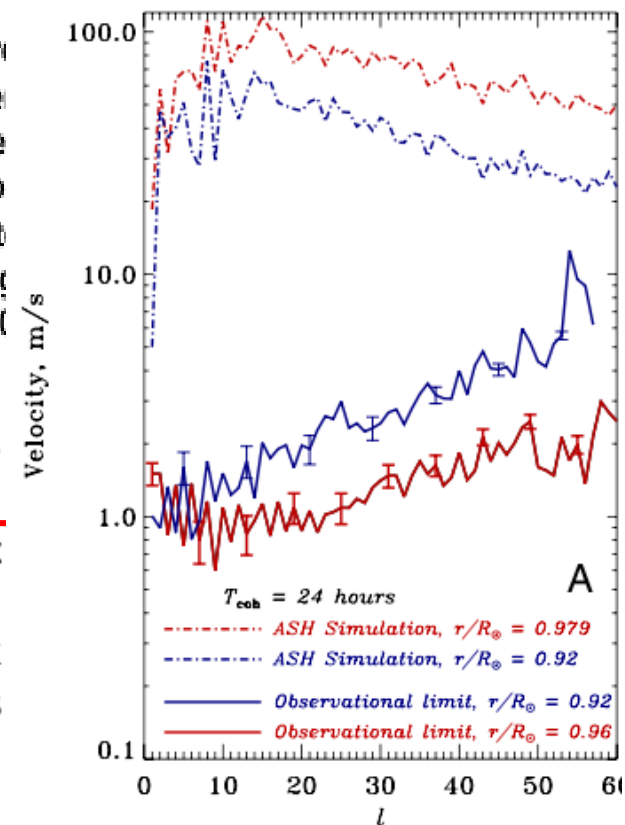
^aDepartment of Geosciences, Princeton University, NJ 08544; ^bMax-Planck-Institut für Sonnensystemforschung

^cSolar Physics Laboratory, National Aeronautics and Space Administration (NASA)/Goddard Space Flight Center of Mathematical Sciences, New York University, NY 10012

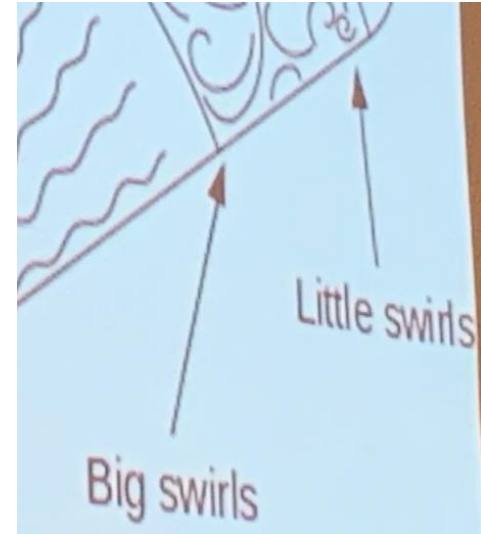
Contributed by Katepalli R. Sreenivasan, May 3, 2012 (sent for review December 30, 2011)

Convection in the solar interior is thought to comprise structure on a spectrum of scales. This conclusion emerges from phenomenological studies and numerical simulations, though neither cover the proper range of dynamical parameters of solar convection. Here, we analyze observations of the wavefield in the solar photosphere using techniques of time-distance helioseismology to image flows in the solar interior. We downsample and synthesize 90

meridional-harmonic degree ℓ . Within the wavenumber band $\ell < 60$, convective velocities are 20–100 times weaker than current theoretical estimates. This constraint suggests the prevalence of a different paradigm of turbulence from that predicted by existing models, prompting the question: what mechanism transports the heat flux of a solar luminosity outwards? Advection is dominated by Coriolis

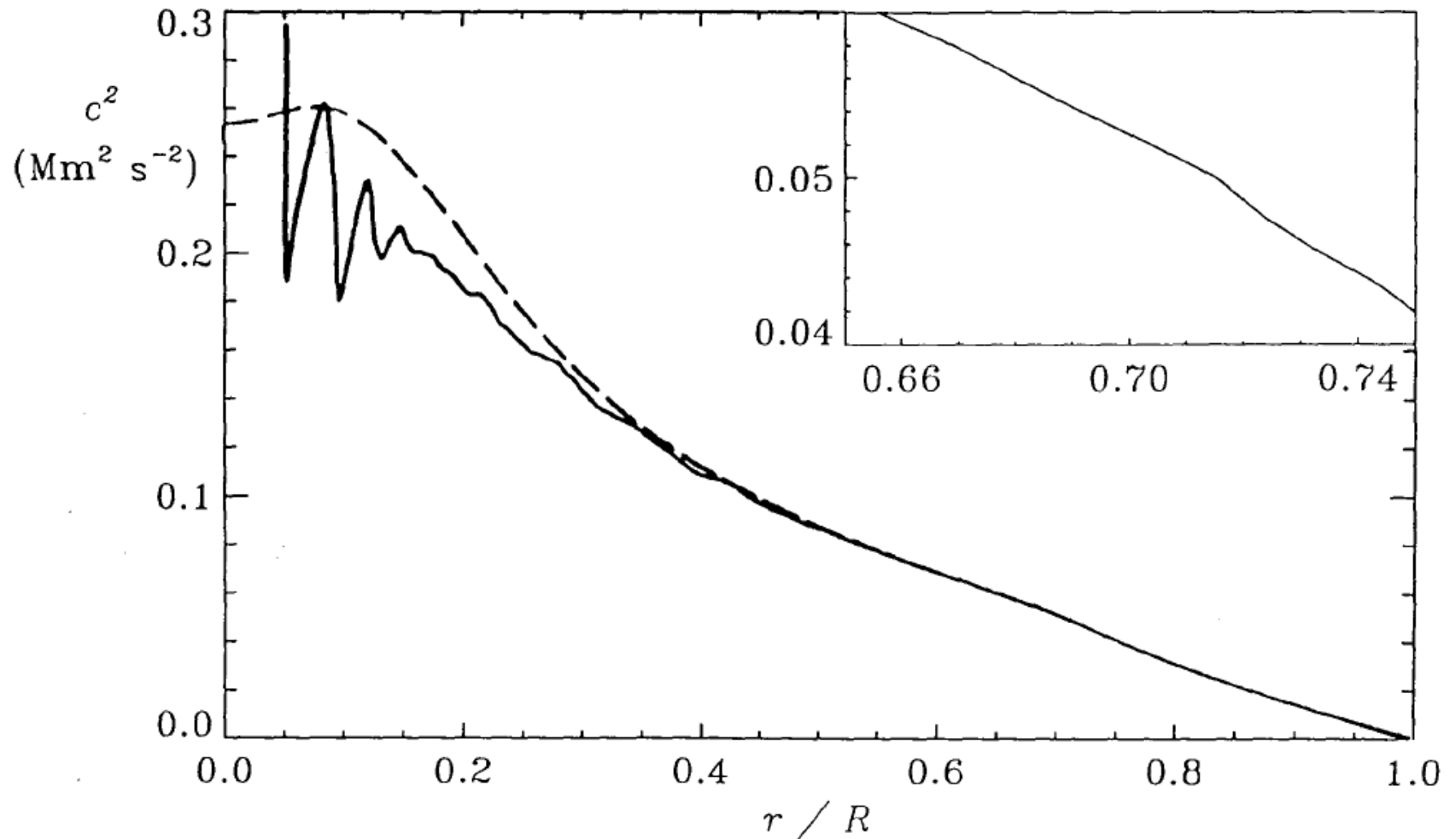


Considerations



- In mixing length theory: $l=H_p$ only hypothesis
- Simulations: subgrid scale diffusion, viscosity
- Envisage reasons for (i) smaller scale flows and/or (ii) deeper parts subadiabatic?
- Convection zone still 200 Mm

Helioseismology: change at $0.7R$



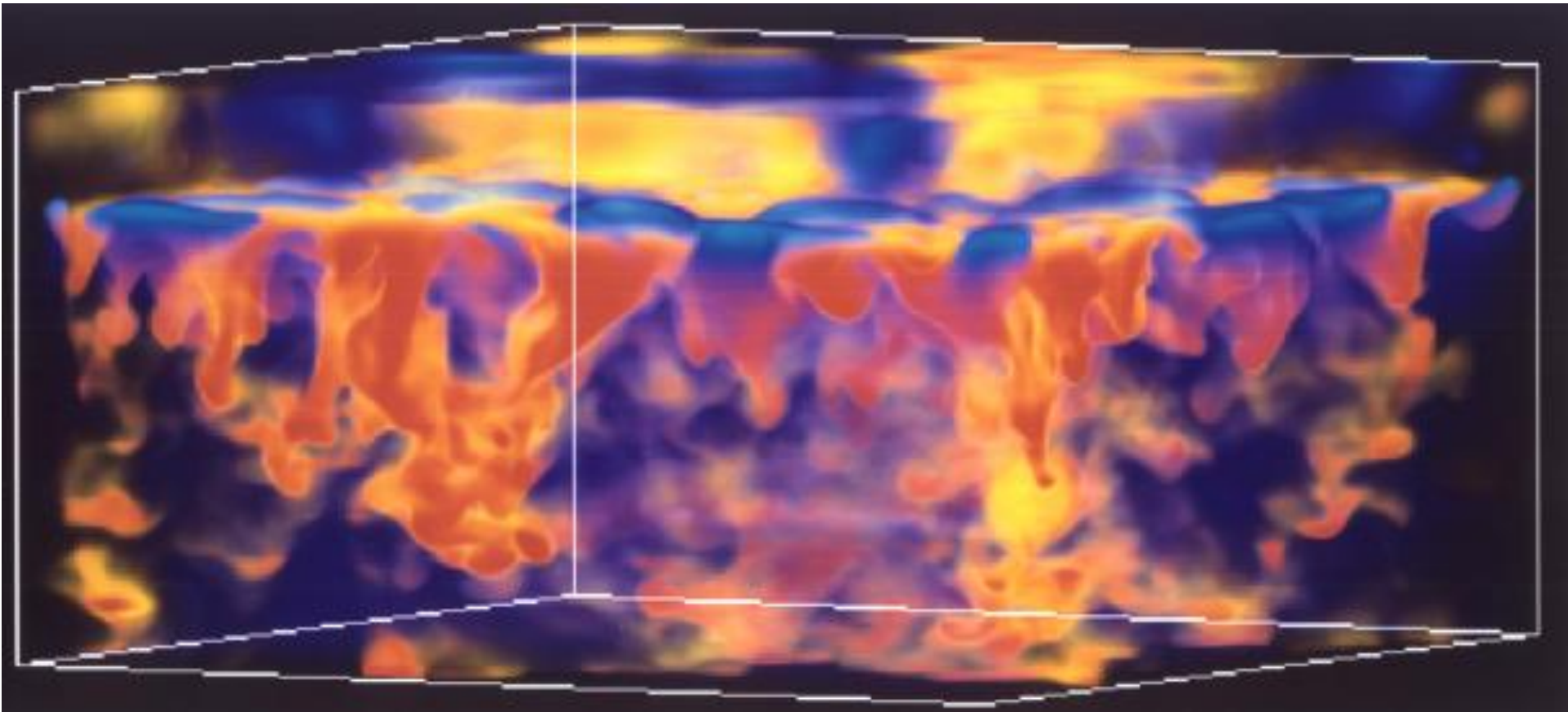
CONVECTION IN STELLAR ENVELOPES: A CHANGING PARADIGM

H.C. SPRUIT

Max Planck Institute for Astrophysics, Garching, Germany

ABSTRACT. Progress in the theory of stellar convection over the past decade is reviewed. The similarities and differences between convection in stellar envelopes and laboratory convection at high Rayleigh numbers are discussed. Direct numerical simulation of the solar surface layers, with no other input than atomic physics, the equations of hydrodynamics and radiative transfer is now capable of reproducing the observed heat flux, convection velocities, granulation patterns and line profiles with remarkably accuracy. These results show that convection in stellar envelopes is an essentially non-local process, being driven by cooling at the surface. This differs distinctly from the traditional view of stellar convection in terms of local concepts such as cascades of eddies in a mean superadiabatic gradient. The consequences this has for our physical picture of processes in the convective envelope are illustrated with the problems of sunspot heat flux blocking, the eruption of magnetic flux from the base of the convection zone, and the Lithium depletion problem.

Stein & Nordlund (1998) simulations



Filamentary, nonlocal

shown: entropy fluctuations **pos** **neg**

Entropy rain

The first consequence of the extreme asymmetry between top and bottom is that upward moving fluid is isentropic, hence neutrally buoyant, all the way from the base of the convection zone to the thermal boundary layer at the top. It follows that we can not say anymore that the flow is driven by buoyant bubbles moving up from below. All driving (in terms of actual forces) is due to cooling at the surface. The gently rising isentropic upflow gets exposed to the cold universe in a thin layer near optical depth unity. The extreme temperature dependence of the opacity makes the cooling happen even faster than it would have done otherwise: as the fluid cools, it becomes more transparent, and cools even faster. The cooled fluid has strong (negative) buoyancy, and collects in a downward flowing lane. On its way down the lanes very soon break up into threads or 'raindrops'. The upward flow of the hot fluid serves to replace the fluid 'condensing' at the top. The entropy contrast of the downflows, the horizontal and vertical velocities, the length scales of the upwellings are all determined by the physics happening in the surface boundary layer.

Tau approximation

$$\dot{s} = -u_j \nabla_j \bar{S} + N_s$$

$$\dot{u}_i = g_i s / c_p + N_u$$

$$\frac{\partial F_i}{\partial t} \propto \overline{u_i \dot{s}} + \overline{\dot{u}_i s} = -\overline{u_i u_j} \nabla_j \bar{S} + \overline{g_i s^2} / c_p + N_{su}$$

Closure
hypothesis

$$N_{su} = -\frac{F_i}{\tau}$$

Theoretical Expression for the Countergradient Vertical Heat Flux

J. W. DEARDORFF

National Center for Atmospheric Research, Boulder, Colorado 80302

A theoretical expression is derived from the heat-flux conservation equation for the counter potential-temperature gradient that can sustain an upward flux of sensible heat. This gradient is found to be $\gamma_c = (g/\theta) \langle \theta'^2 \rangle / \langle w'^2 \rangle$, where $\langle \theta'^2 \rangle$ is the potential temperature variance and $\langle w'^2 \rangle$ is the vertical velocity variance. The usual down-gradient eddy coefficient expression for the heat flux is obtained from the derivation only if γ_c is set to zero. Aircraft measurements of $(g/\theta) \langle \theta'^2 \rangle / \langle w'^2 \rangle$ in the middle and upper portions of convective planetary boundary layers indicate that this expression for γ_c is of the same order of magnitude (near $0.7 \times 10^{-5} \text{ }^\circ\text{K cm}^{-1}$) as the value deduced previously for γ_c from completely different considerations.

Evidence has been accumulating for many years that in the central half or so of the planetary boundary layer (PBL) under conditions of upward sensible heat flux the lapse rate is slightly less than adiabatic; that is, the heat flux is countergradient. The evidence up to 1966 is summarized by Deardorff [1966]. Since that time, additional aircraft observations of both potential temperature and heat flux by Lenschow [1970] and by Warner [1971] demon-

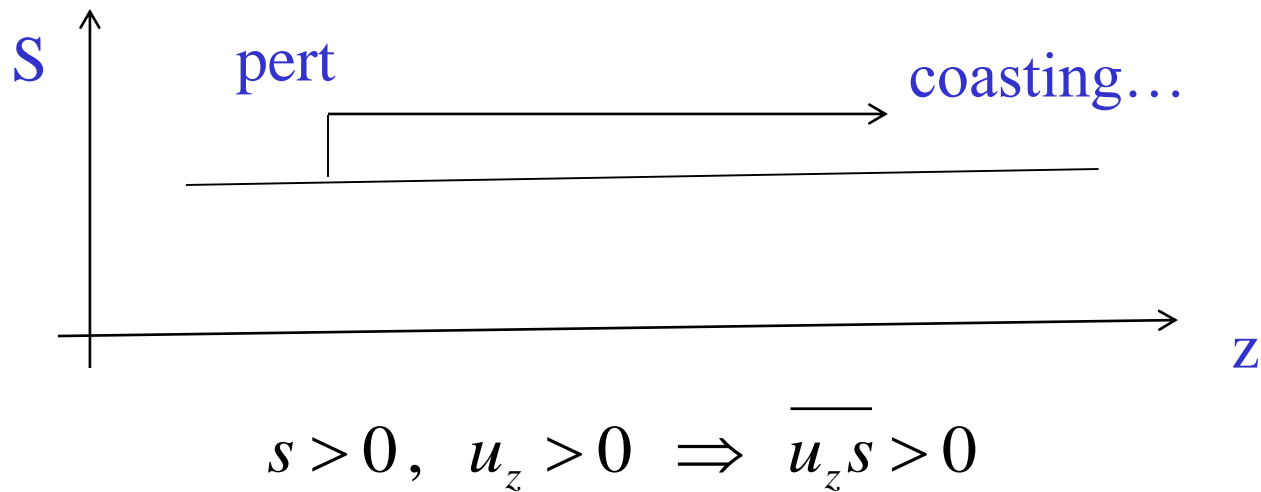
could represent a much larger averaging area or a time or ensemble average. Although this value of γ_c is small, the question of its use is far from being of only academic concern. In a thick PBL of 3 km height, for example, a numerical model that uses equations 1 and 2 will predict values of $\langle \theta \rangle$ at upper levels in the PBL (relative to lower levels) nearly 2°K warmer than one that sets $\gamma_c = 0$ for a given set of external conditions.

et al. [1971], and *Donaldson* [1972] that utilize equations for the second moments and closure assumptions for third moments. The equation, which makes use of the Boussinesq approximation, is

$$\begin{aligned}
 \frac{\partial}{\partial t} \langle w' \theta' \rangle = & -\langle u_i \rangle \frac{\partial}{\partial x_i} \langle w' \theta' \rangle - \langle w' u_i' \rangle \frac{\partial \langle \theta \rangle}{\partial x_i} \\
 & - \langle u_i' \theta' \rangle \frac{\partial \langle w \rangle}{\partial x_i} - \frac{\partial}{\partial x_i} \langle w' u_i' \theta' \rangle \\
 & + \frac{g}{\theta_0} \langle \theta'^2 \rangle - \frac{1}{\rho_0} \left\langle \theta' \frac{\partial p'}{\partial z} \right\rangle
 \end{aligned} \tag{3}$$

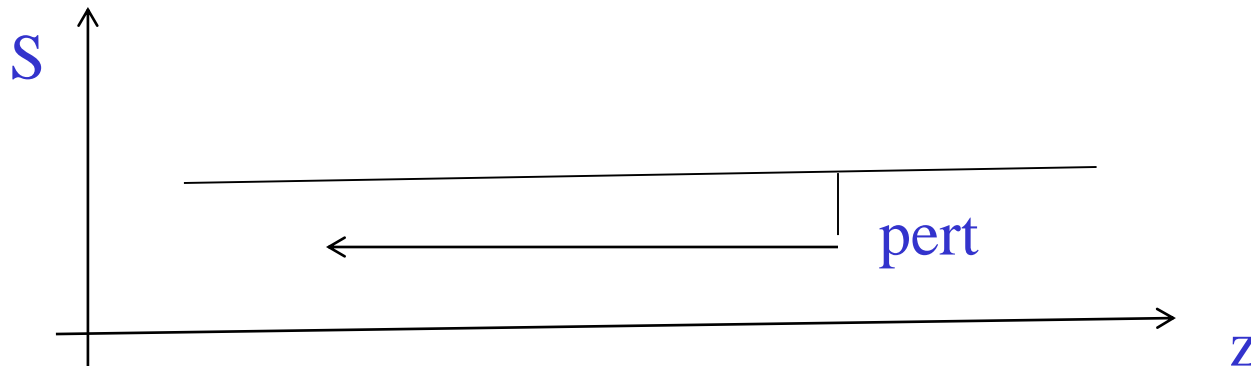
Physical meaning?

$$s / c_p = \frac{1}{\gamma} \ln p - \ln \rho$$



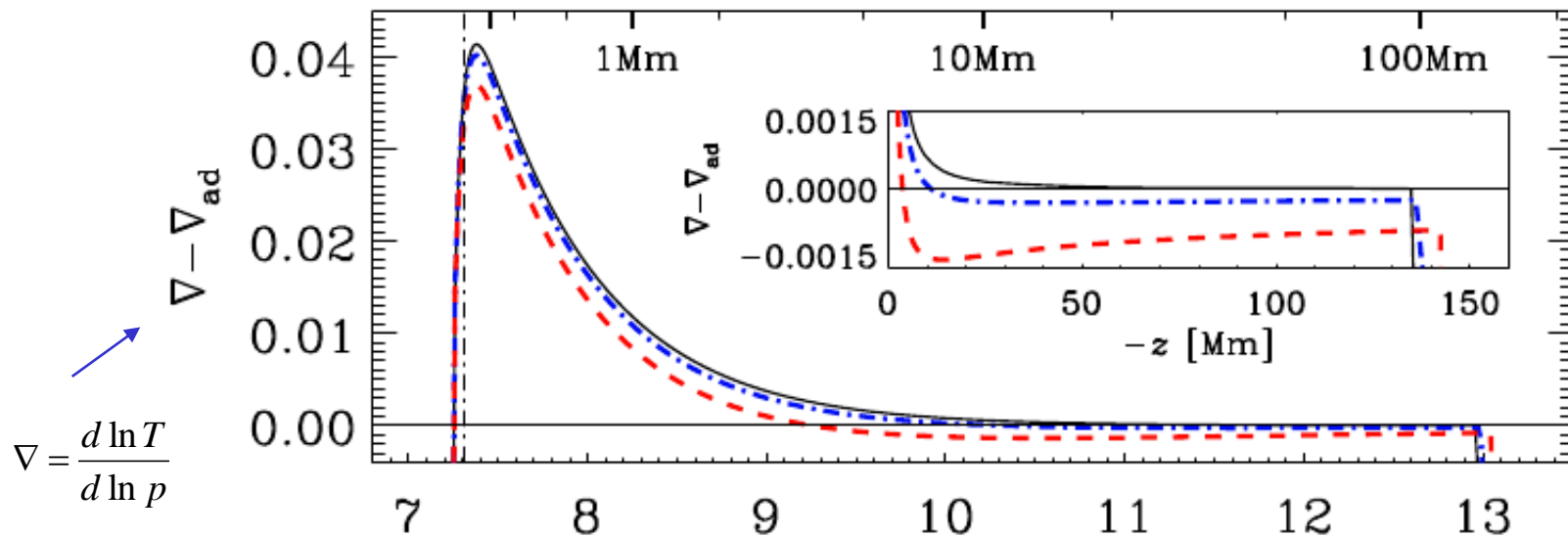
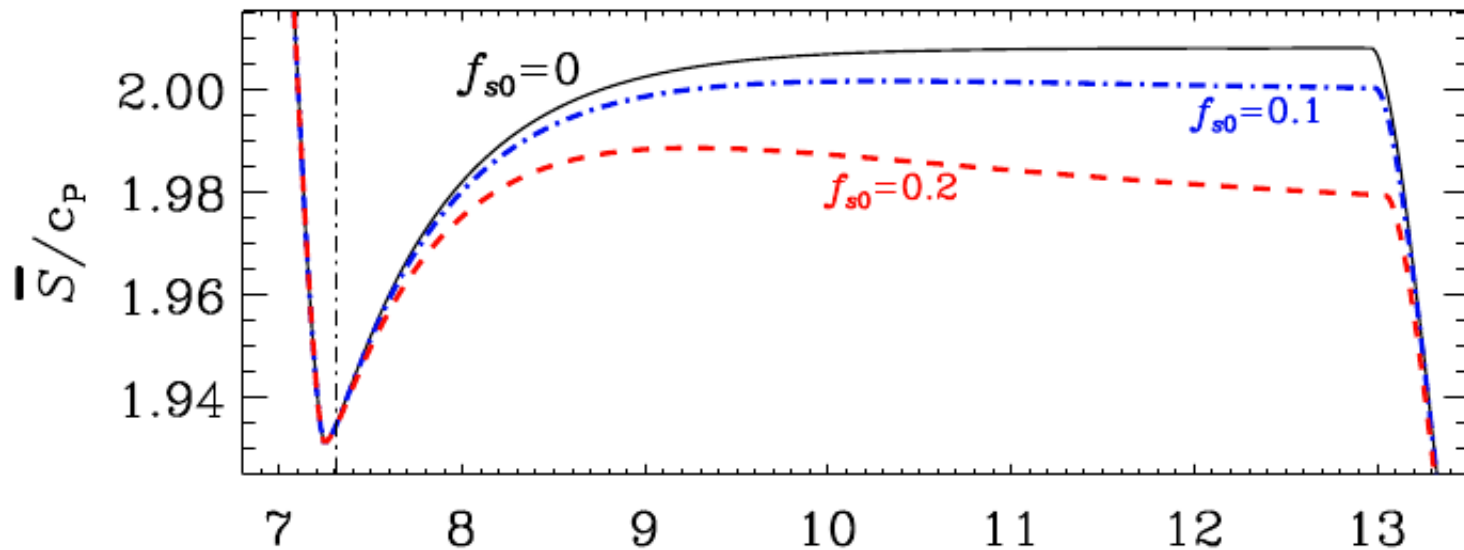
Physical meaning?

$$s / c_p = \frac{1}{\gamma} \ln p - \ln \rho$$



$$s < 0, \quad u_z < 0 \quad \Rightarrow \quad \overline{u_z s} > 0$$

New solutions with Deardorff flux



Gradient & Deardorff terms

$$\mathbf{F}_G = -\frac{1}{3}\tau_{\text{red}} u_{\text{rms}}^2 \bar{\rho} \bar{T} \nabla \bar{S},$$

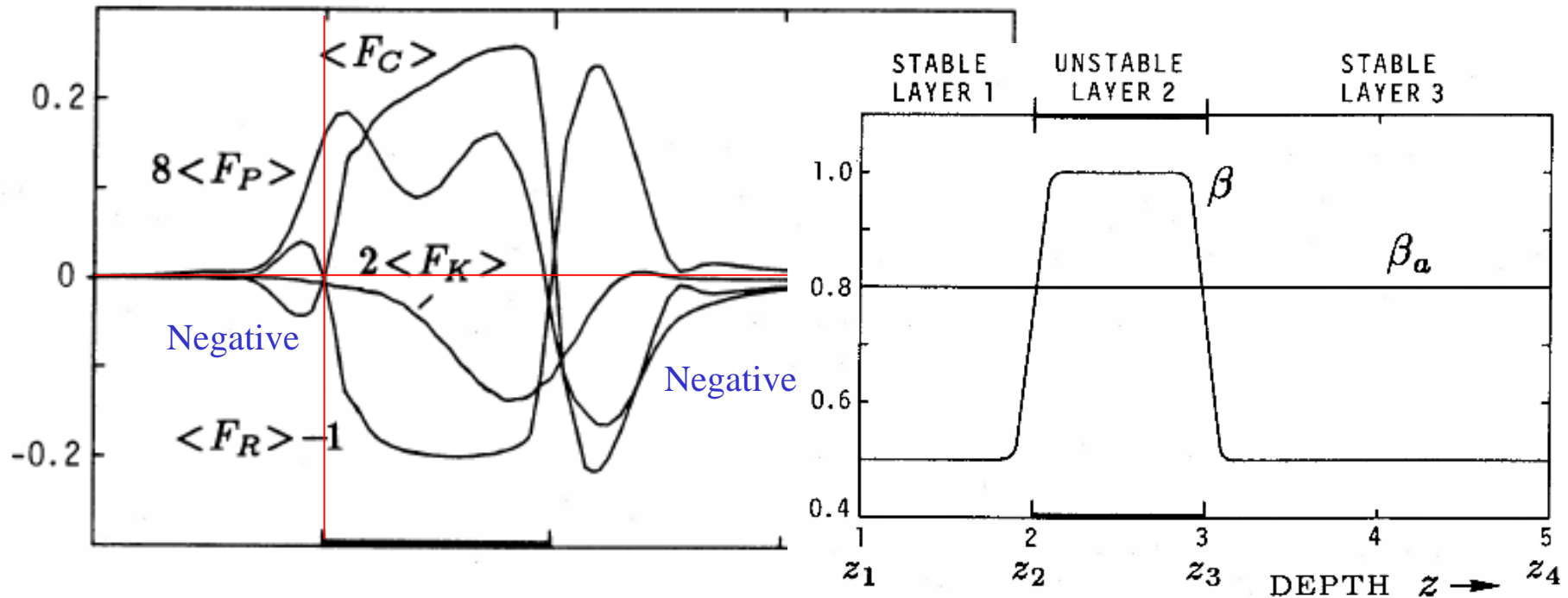
$$\mathbf{F}_D = -\tau_{\text{red}} \overline{s^2} \mathbf{g} \bar{\rho} \bar{T} / c_P$$

extra nabla term in standard MLT

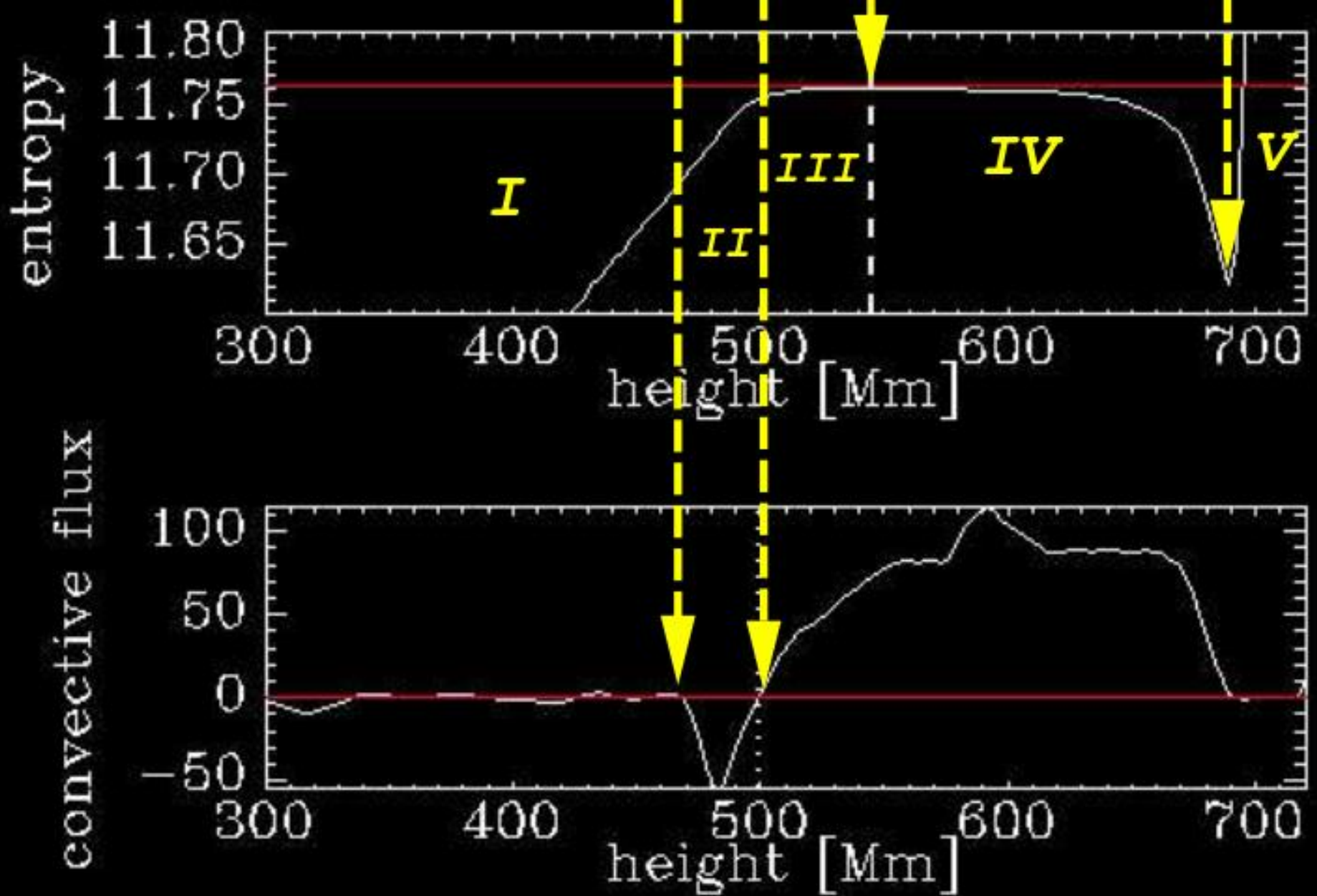
$$F_{\text{enth}} = \frac{1}{3} \bar{\rho} c_P \bar{T} (\tau_{\text{red}} u_{\text{rms}}^2 / H_P) (\nabla - \nabla_{\text{ad}} + \nabla_D)$$

Subadiabaticity of the deeper layers

previously taboo, by construction



Hurlburt, Toomre, & Massaguer (1986)



Brandenburg, Nordlund, & Stein (2000) using Kramers opacity

Hydrostatics with $K(z) \rightarrow K(\rho, T)$

Radiative flux:

$$\mathbf{F}_{\text{rad}} = -K \nabla T \quad \text{with} \quad K = \frac{16\sigma_{SB}T^3}{3\kappa\rho}$$

Kramers' opacity: $\kappa = \kappa_0 (\rho/\rho_0)^a (T/T_0)^b$

Nonconvecting solution ($F_{\text{rad}} = \text{const}$, $T_{\text{top}} = 0.84T_{\text{eff}}$)

$$(T/T_0)^{4+a-b} = (n+1) \nabla_{\text{rad}}^{(0)} (P/P_0)^{1+a} + (T_{\text{top}}/T_0)^{4+a-b}$$

Brandenburg (2016)

Polytropic index:

$$n = \frac{3-b}{1+a} = \frac{3+3.5}{1+1} = 3.25 \quad > 1.5 (\rightarrow \text{stable})$$

But why optically thick = thin in equilibrium?

The equation of radiative transfer is

$$\hat{\mathbf{n}} \cdot \nabla I = -\kappa \rho (I - S). \quad (1)$$


where $I = I(\mathbf{x}, t, \hat{\mathbf{n}}, \nu)$ is the intensity, ρ is the density, κ is the intensity, and $S = (\sigma_{\text{SB}}/\pi) T^4$ is the source function.

Equation (1) can be solved by taking moments. We define 0th, 1st, and 2nd moments as follows,

$$J = \frac{1}{4\pi} \int_{4\pi} I \, d\Omega, \quad (2)$$

$$\mathbf{F} = \int_{4\pi} I \hat{\mathbf{n}} \, d\Omega, \quad (3)$$

$$\mathbf{P} = \frac{1}{4\pi} \int_{4\pi} I \hat{\mathbf{n}} \hat{\mathbf{n}} \, d\Omega. \quad (4)$$

CONTACT Axel Brandenburg  |
Dedicated to Professor Ed A. Spiegel

the 0th and 1st moment of Equation (1)

$$\nabla \cdot \mathbf{F} = -4\pi \kappa \rho (J - S),$$

$$\nabla \cdot \mathbf{P} = -\frac{\kappa \rho}{4\pi} \mathbf{F}.$$

Making the closure assumption

$$P_{ij} = \frac{1}{3} \delta_{ij} J.$$

Equation (6) becomes

$$\frac{1}{3} \nabla J = -\frac{\kappa \rho}{4\pi} \mathbf{F}.$$

$$\rho T \frac{DS}{Dt} = \nabla \cdot \frac{4\pi}{3\kappa \rho} \nabla J,$$

instead of

$$\rho T \frac{DS}{Dt} = \nabla \cdot \frac{4\pi}{3\kappa \rho} \nabla S \equiv \nabla \cdot K \nabla T.$$

...end of a generation has begun



1932-2020

**Magnetic activity and
variations in solar luminosity**

E. A. Spiegel

Department of Astronomy, Columbia University, New York,
New York 10027

N. O. Weiss*

Harvard-Smithsonian Center for Astrophysics, Cambridge,
Massachusetts 02138

...end of a generation has begun



1932-2020

Magnetic activity and variations in solar luminosity

E. A. Spiegel

Department of Astronomy, Columbia University, New York, New York 10027

N. O. Weiss*

Harvard-Smithsonian Center for Astrophysics, Cambridge, Massachusetts 02138



1935-2020

chr. / AN 335, No. 5, 459 – 469 (2014) / DOI 10.1002/asna.2

Mean-field dynamos: The old concept

Karl Schwarzschild Award Lecture 2013

K.-H. Rädler*

Leibniz-Institut für Astrophysik, An der Sternwarte 16, D-14482

Received 2014 Apr 7, accepted 2014 Apr 10

Published online 2014 Jun 2

Key words magnetic fields – magnetohydrodynamics (MHD)



1943-2020

Mon. Not. R. Astron. Soc. 275, 191–194 (1995)

On the generation of bisymmetric galaxies by tidal interactions

David Moss

Department of Mathematics, The University, Oxford Rd, Manchester M13

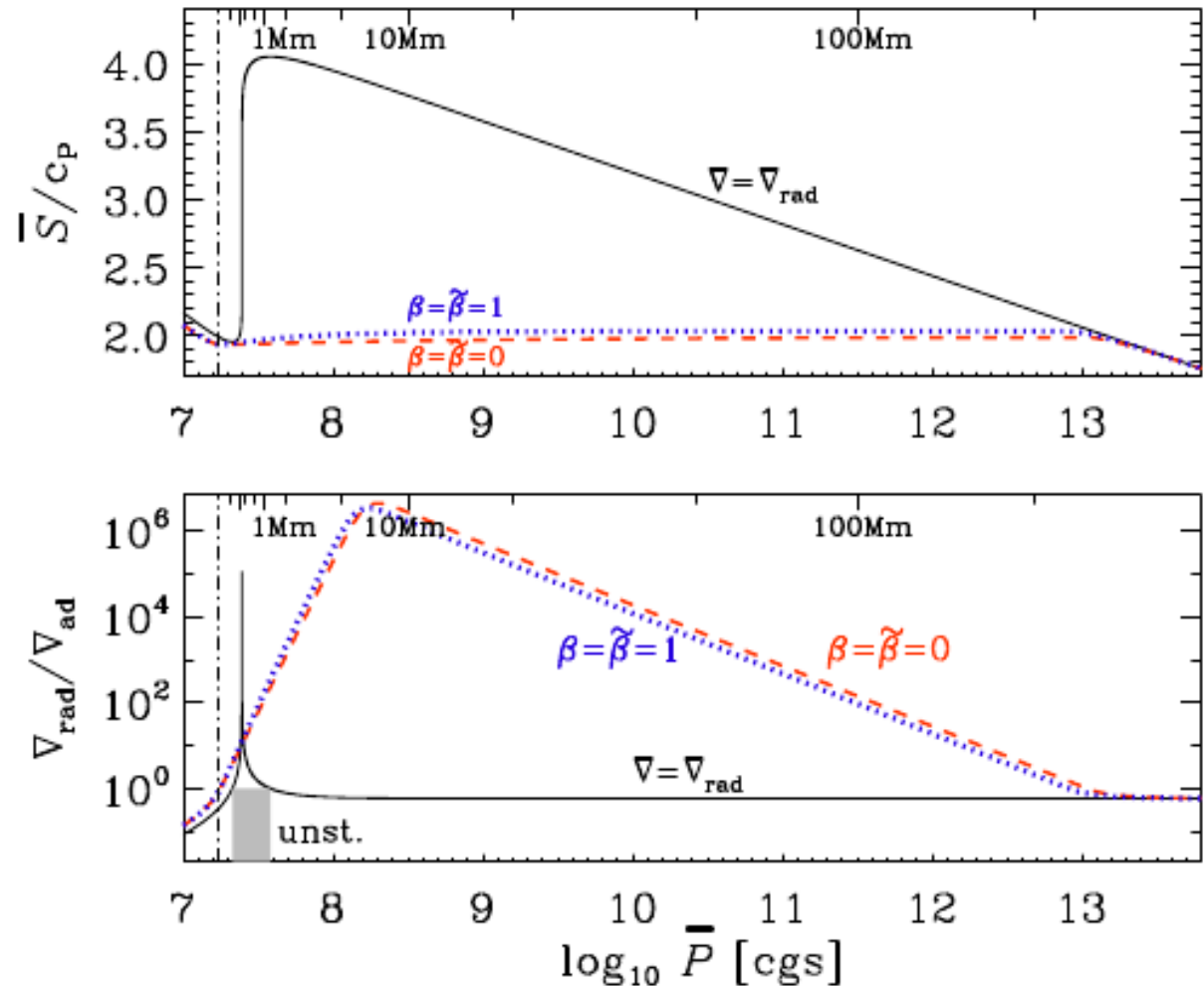
Accepted 1995 March 2. Received 1994 September 23

Solar non-convecting model

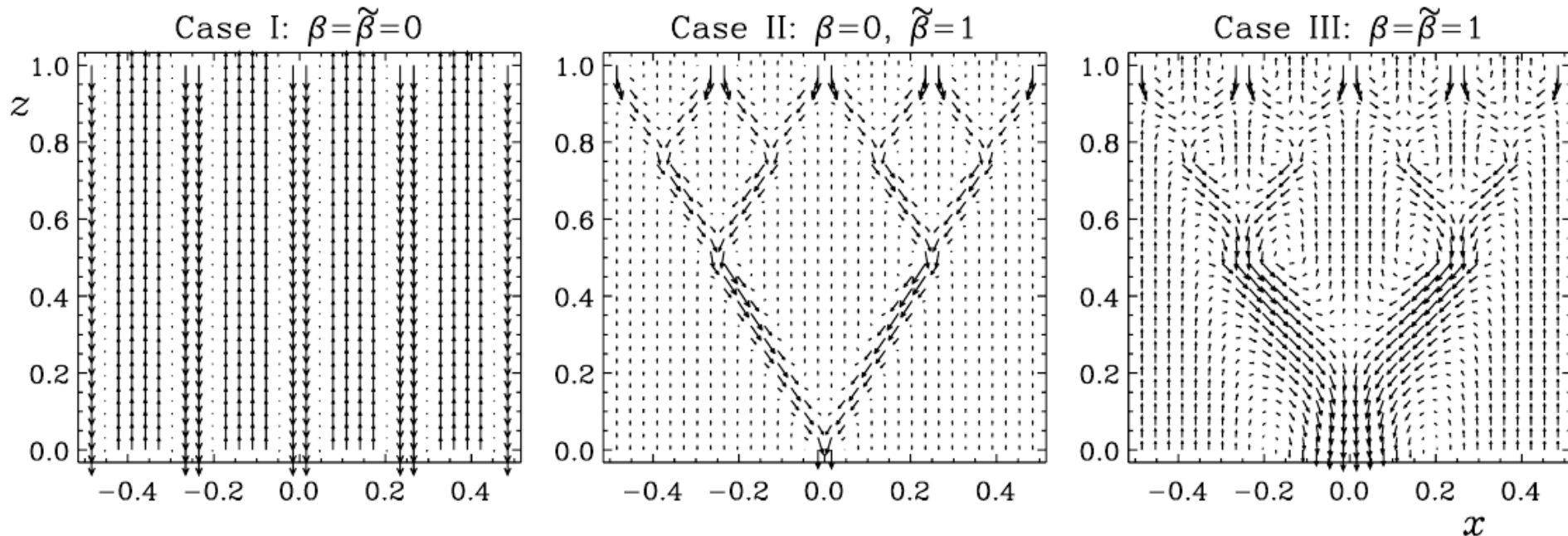
- Unstable layer extremely thin (1Mm)
- But extremely unstable
- Deep layers will be mixed by long nonlocal spoon
- $\rightarrow S \sim \text{const}$

Brandenburg (2016)

large structures
 \rightarrow not excited!



Thickness versus separation



$$F_{\text{enth}} \propto u_{\text{rms}}^3 (k_{f0} H_P)^{1-\beta}$$

$$F_{\text{enth}} \propto u_{\text{rms}} \Delta \nabla / (k_{f0} H_P)^{1-\tilde{\beta}}$$

$$u_{\text{rms}} \propto (\Delta \nabla)^{1/2} / (k_{f0} H_P)^{1-\beta'}$$

$$F_{\text{enth}} \propto (\Delta \nabla)^{3/2} / (k_{f0} H_P)^{2(1-\beta'')}$$

$$F_{\text{kin}} \propto (\Delta \nabla)^{3/2} / (k_{f0} H_P)^{3(1-\beta')}$$

buoyancy force

mean-field expression

$$\beta' = (\beta + \tilde{\beta})/2$$

$$\beta'' = (\beta' + \tilde{\beta})/2 = (\beta + 3\tilde{\beta})/4$$

kinetic energy flux

Nonconvecting 1-D atmospheres

- Solve from the bottom upward

$$d \ln \bar{P} / dz = -\bar{\rho}g / \bar{P},$$

$$d \ln \bar{T} / dz = -F / K\bar{T}.$$

$$\nabla = d \ln \bar{T} / d \ln \bar{P} = F\bar{P} / K\bar{T} \bar{\rho}g = Fc_P \nabla_{\text{ad}} / Kg,$$

$$d \ln \bar{T} / d \ln \bar{P} = \nabla,$$

$$-z = \int H_P d \ln \bar{P} \quad \text{and} \quad \tau = \int (\kappa \bar{P} / g) d \ln \bar{P},$$

Solutions

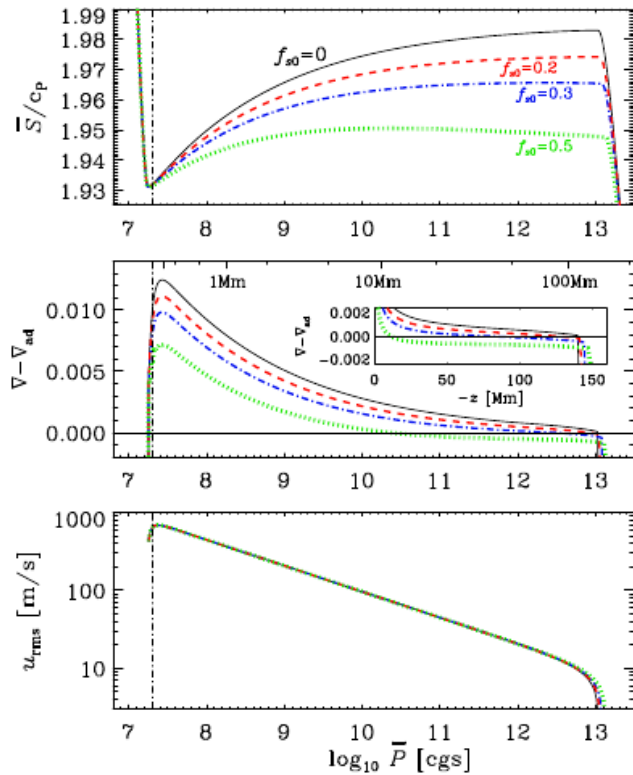


Figure 4. Profiles of \bar{S}/c_p , $\nabla - \nabla_{\text{ad}}$, and u_{rms} for $f_{s0} = 0$ ($\nabla_D = 0$), as well as $f_{s0} = 0.2, 0.3$, and 0.5 for $\beta = \bar{\beta} = 0$ (Case I) with $\bar{\zeta} = 1/9$. The location of the surface ($\tau = 1$) is indicated by vertical dashed-dotted lines and geometric depths below the surface are indicated in the middle panel, starting with tick marks at 100, 200, and 500 km, and continuing with 1, 2, and 5 Mm, etc. The inset in the middle panel shows $\nabla - \nabla_{\text{ad}}$ over a narrower range as a function of $-z$.

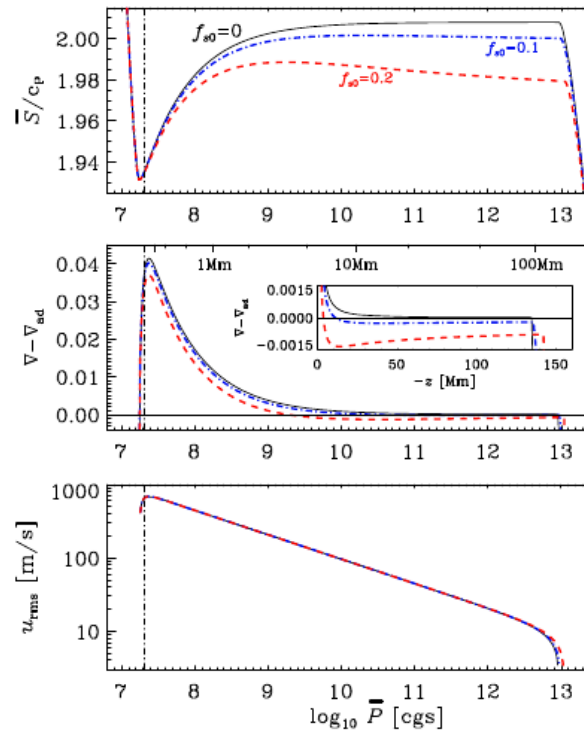


Figure 5. Same as Figure 4, but for $\beta = 0$, $\bar{\beta} = 1$ (Case II) with $\bar{\zeta} = 1/9$, and $f_{s0} = 0, 0.1$, and 0.2 .

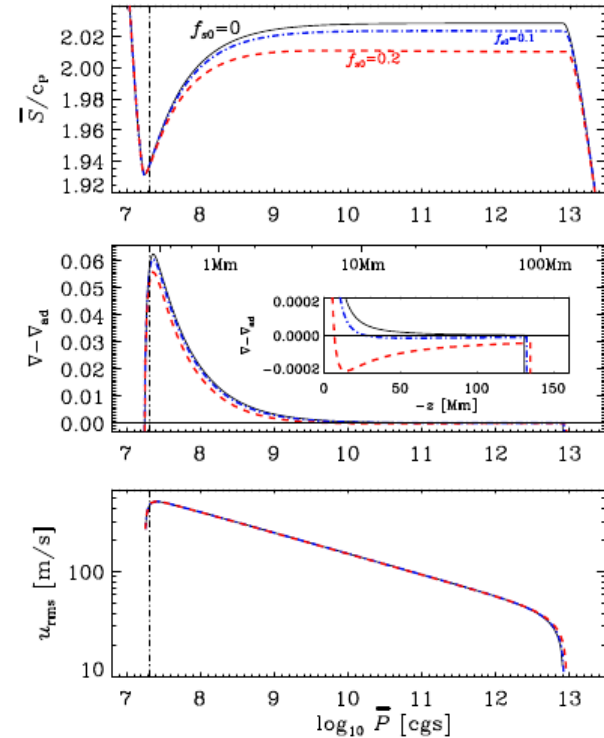


Figure 6. Same as Figure 4, but for $\beta = \bar{\beta} = 1$ (Case III) $\bar{\zeta} = 1/3$, and $f_{s0} = 0, 0.1$, and 0.2 .

Equation (48), we find $\text{Ma} \propto \bar{T}^{-m}$

$$m = 1 - \beta' + (1/2 + \beta'')/\xi.$$

$$u_{\text{rms}} \propto \bar{P}^{(1-2m)/5} = \bar{P}^{-1/3}$$

$$u_{\text{rms}} \propto \bar{P}^{(1-2m)/5} = \bar{P}^{-1/5}$$

always: $F_{\text{tot}} = F_{\text{conv}} + F_{\text{rad}}$

here: $F_{\text{conv}} = F_{\text{enth}} + F_{\text{kin}}$

Kinetic energy flux

$$F_{\text{kin}} = -\phi_{\text{kin}} \bar{\rho} u_{\text{rms}}^3$$

f	1/2	1/3	0.14	0.015	0.0006
ϕ_{kin}	0	0.35	1	4	20
$-\bar{U}_{\downarrow}/u_{\text{rms}}$	1	1.4	2.5	8	40
$\bar{U}_{\uparrow}/u_{\text{rms}}$	1	0.7	0.4	0.12	0.025

Self-consistency &
upflow estimate

$$-H_P \frac{d\bar{S}/c_P}{dz} = \frac{(\Delta S)_0}{c_P} \frac{df_s}{d \ln \bar{P}} = \frac{2}{5} \frac{(\Delta S)_0}{c_P} f_s > 0,$$

$$\bar{\rho} \bar{T} \bar{U}_{\uparrow} d\bar{S}_{\uparrow}/dz \approx -(dF_{\text{rad}}/dz)_{\uparrow}.$$

pos pos -(neg)

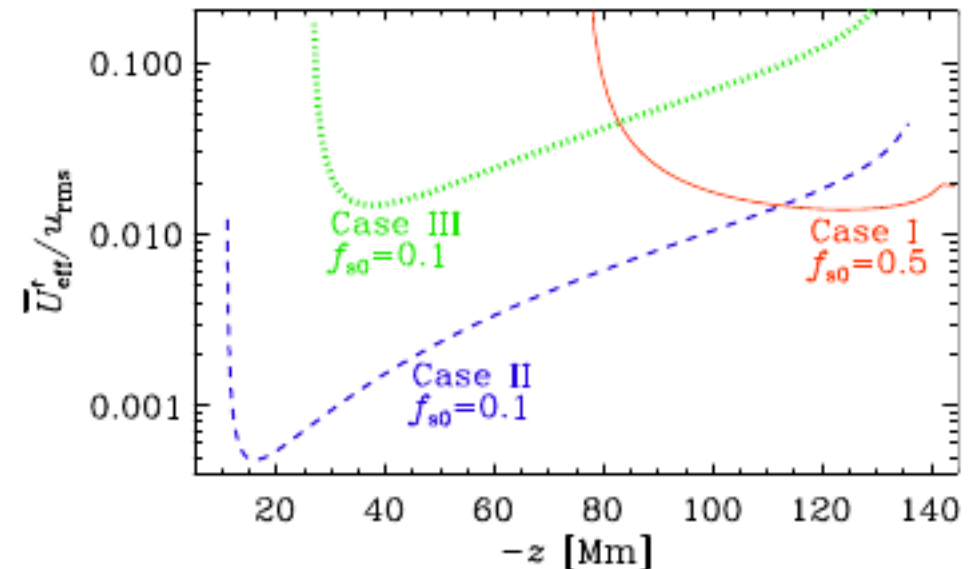
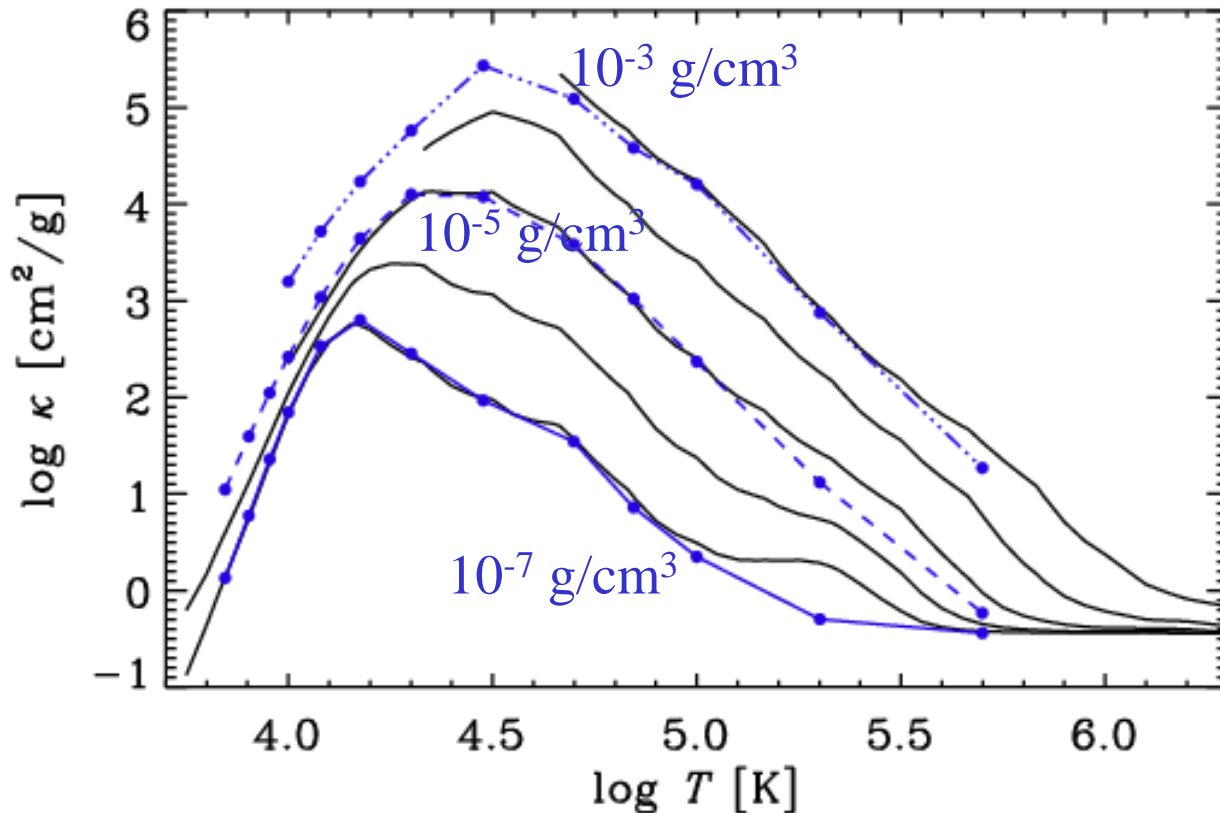


Figure 8. Dependence of $\bar{U}_{\text{eff}}^{\uparrow}/u_{\text{rms}}$ on depths $-z$ for Case I with $f_{s0} = 0.5$ (solid red line), as well as Cases II and III with $f_{s0} = 0.1$ (dashed blue and dotted green lines, respectively).

OPAL vs. old Cox & Stewart opacities



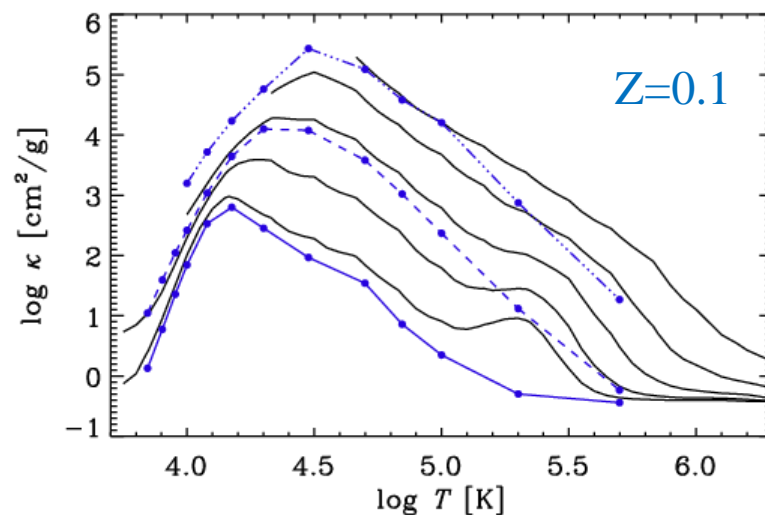
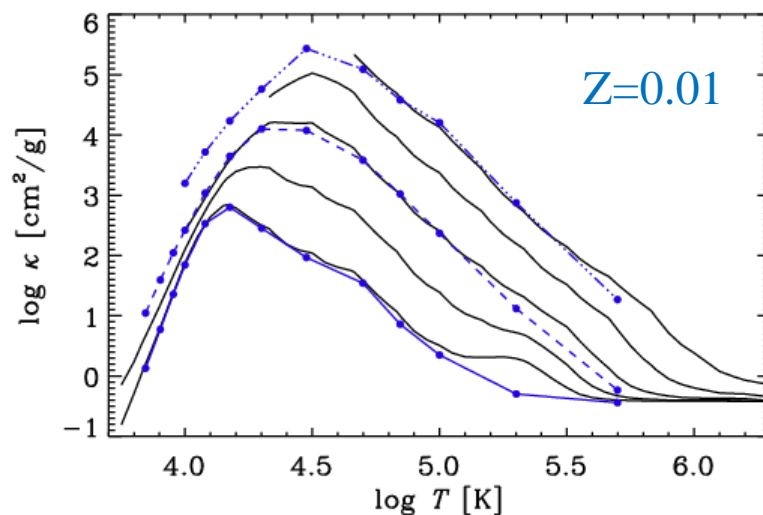
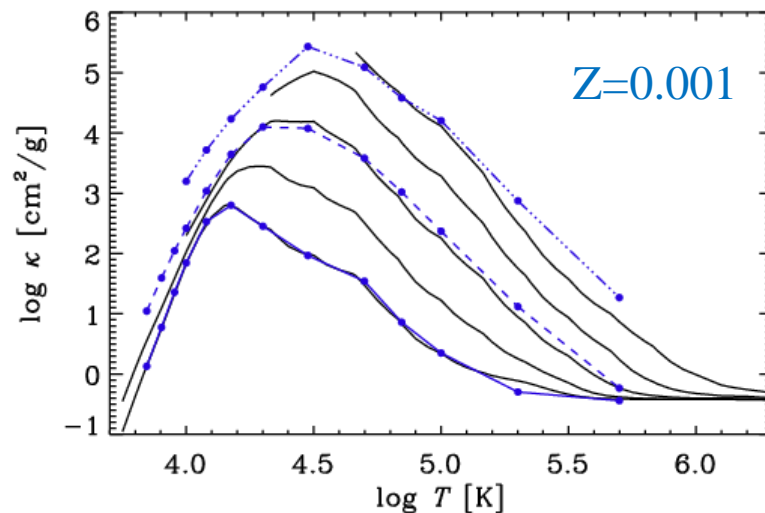
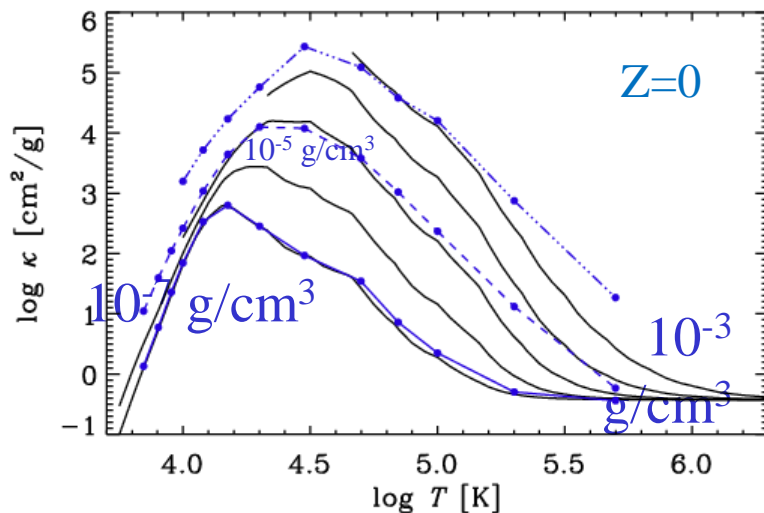
- 2 branches
- Rising branch from H- opacity at low T
- Decreasing branch from bound-free & free-free opacity
- Kramers type opacity

$$\kappa = \kappa_0 \rho^a T^b$$

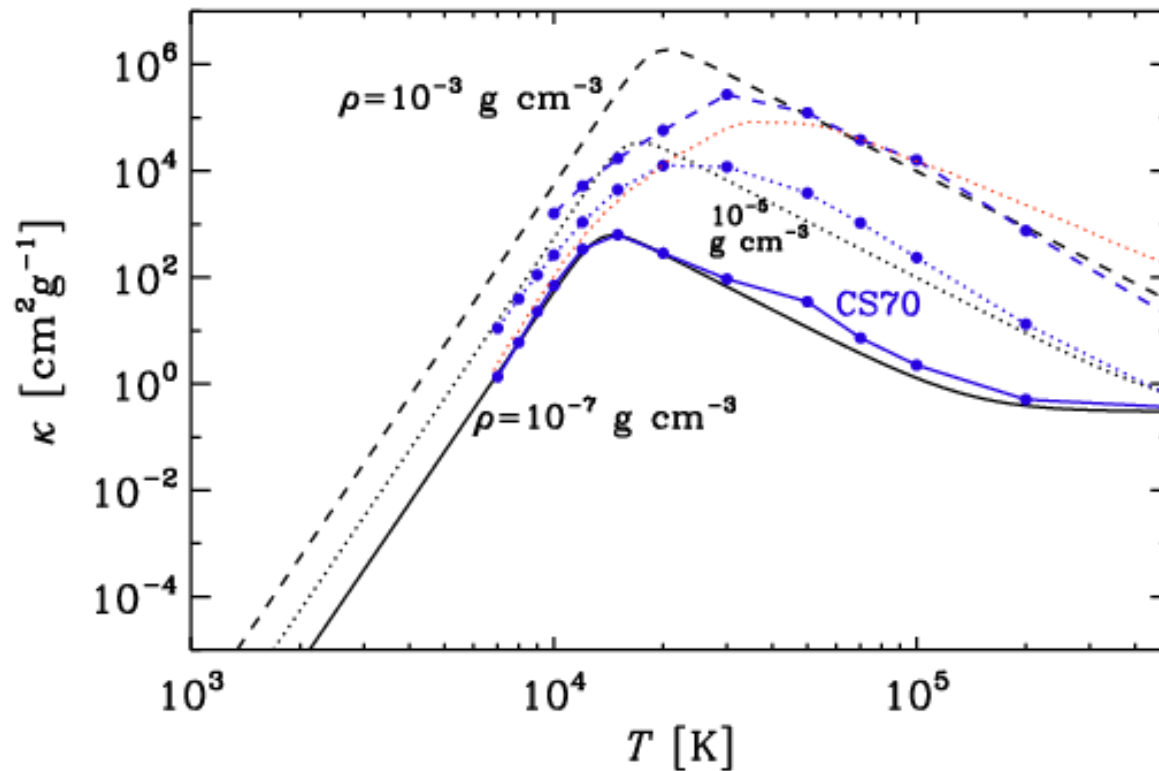
- $a=1, b=-3.5$

Different metallicities

<http://cdsweb.u-strasbg.fr/topbase/home.html>



Essentials captured by analytic formula



$$\kappa^{-1} = \kappa_{\text{Kr}}^{-1} + \kappa_{\text{H}^-}^{-1}$$

$$\kappa = \kappa_0 \rho^a T^b$$

- Kr: $a=1, b=-7/2$
- H⁻: $a=0.5, b=+10\dots$

Solve hydro model with prescribed κ

$$\frac{D \ln \rho}{Dt} = -\nabla \cdot \mathbf{u},$$

$$\rho \frac{D\mathbf{u}}{Dt} = -\nabla P + \rho \mathbf{g} + \nabla \cdot (2\nu \rho \mathbf{S}),$$

$$\rho T \frac{DS}{Dt} = -\nabla \cdot \mathbf{F}_{\text{rad}} + 2\nu \rho \mathbf{S}^2 + \mathcal{H},$$

$$-\nabla \cdot \mathbf{F}_{\text{rad}} = \kappa \rho \oint_{4\pi} (I - S) d\Omega,$$

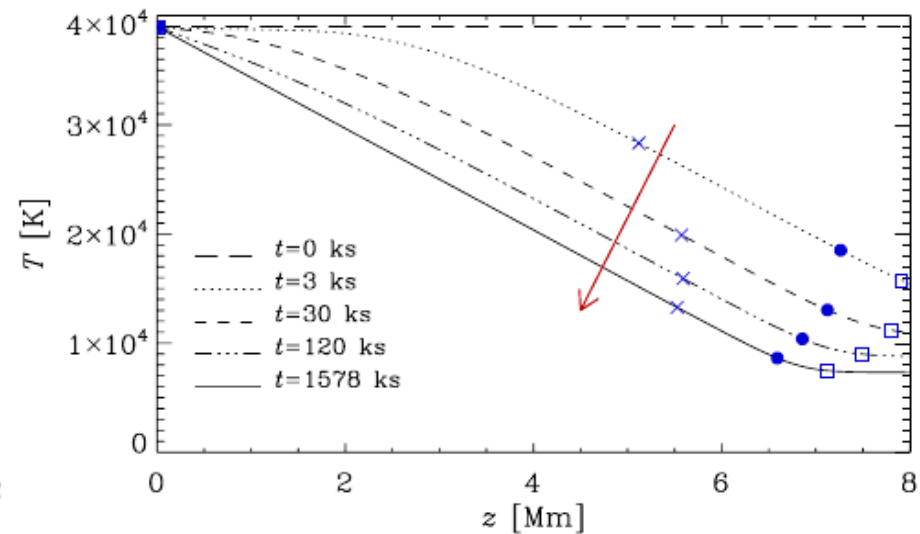
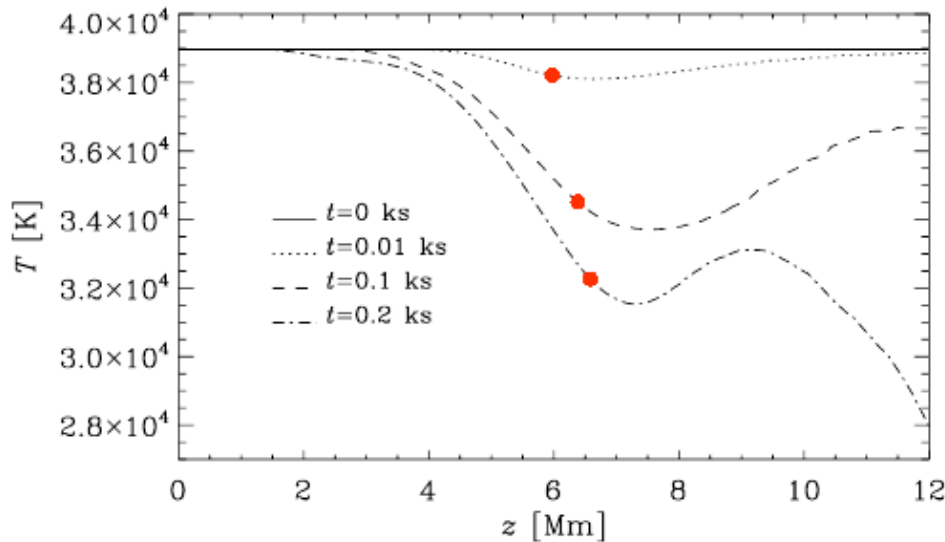
$$-\hat{\mathbf{n}} \cdot \nabla I = \kappa \rho (I - S),$$

- Cartesian
- Gray rad transfer
- 22 – 26 rays in 3D
- 2 rays in 1-D (up/down)

Radiative transfer in decomposed domains★

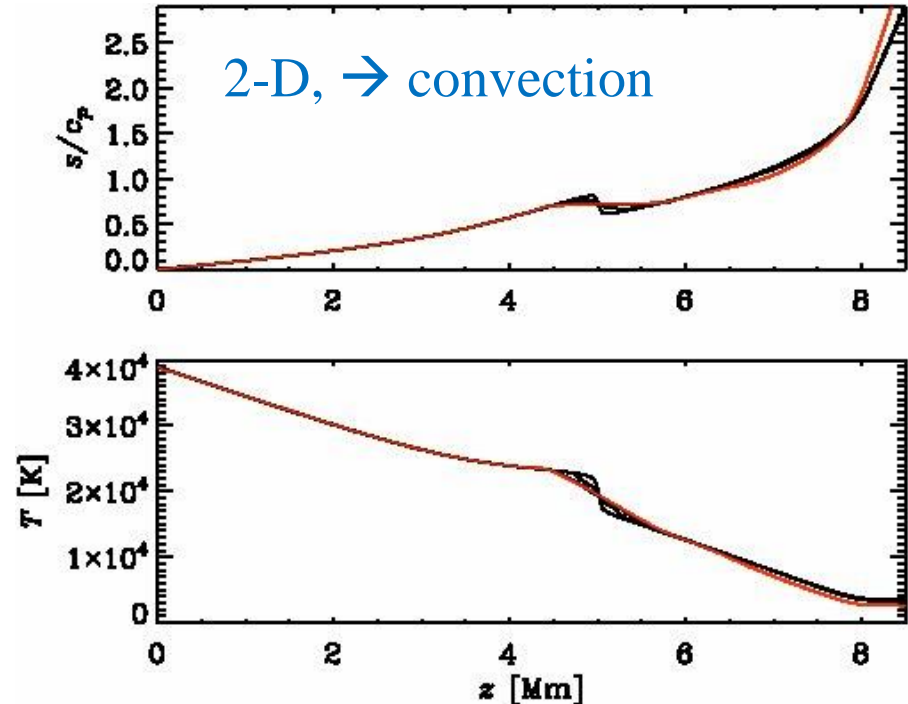
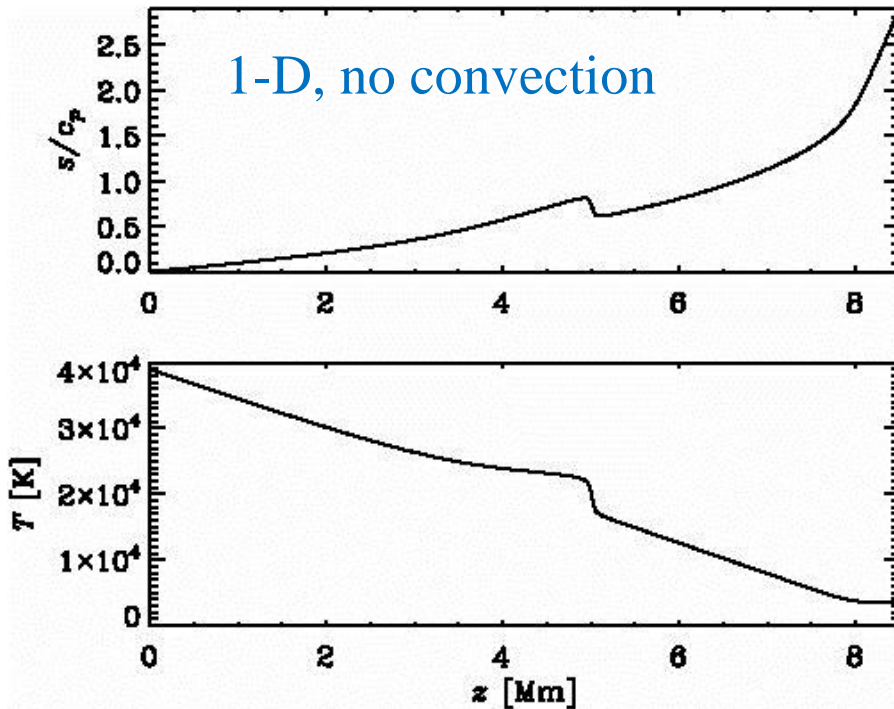
Relaxation from isothermal state

Barekat & Brandenburg (2014, A&A 571, A68)



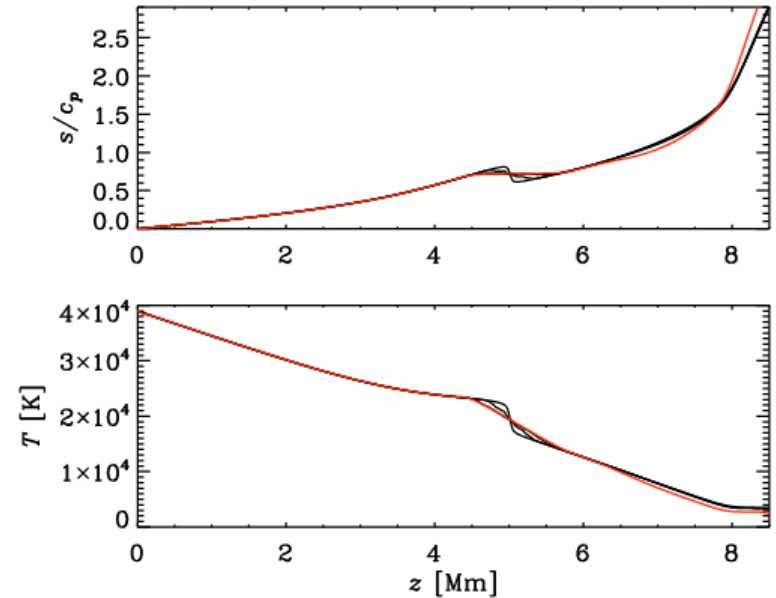
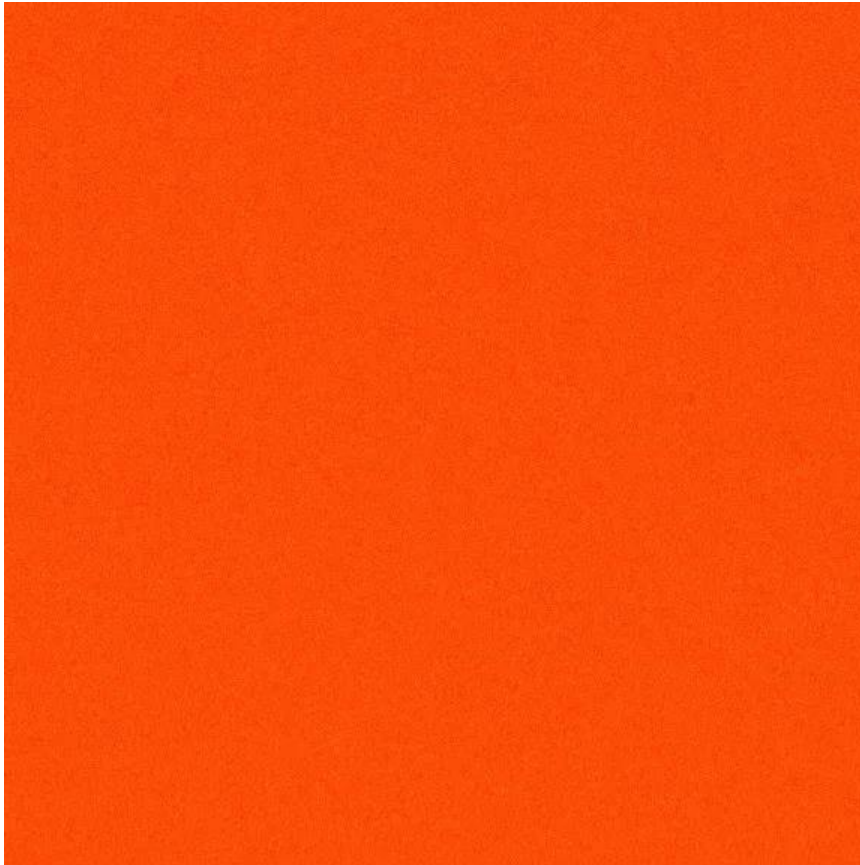
- Most rapid cooling near, or slightly above $\tau=1$
- Relaxation to near-polytropic interior plus isothermal top
- Polytropic index depends on a and b

Constant opacity ($a=b=0$) with exponential (iron) bump



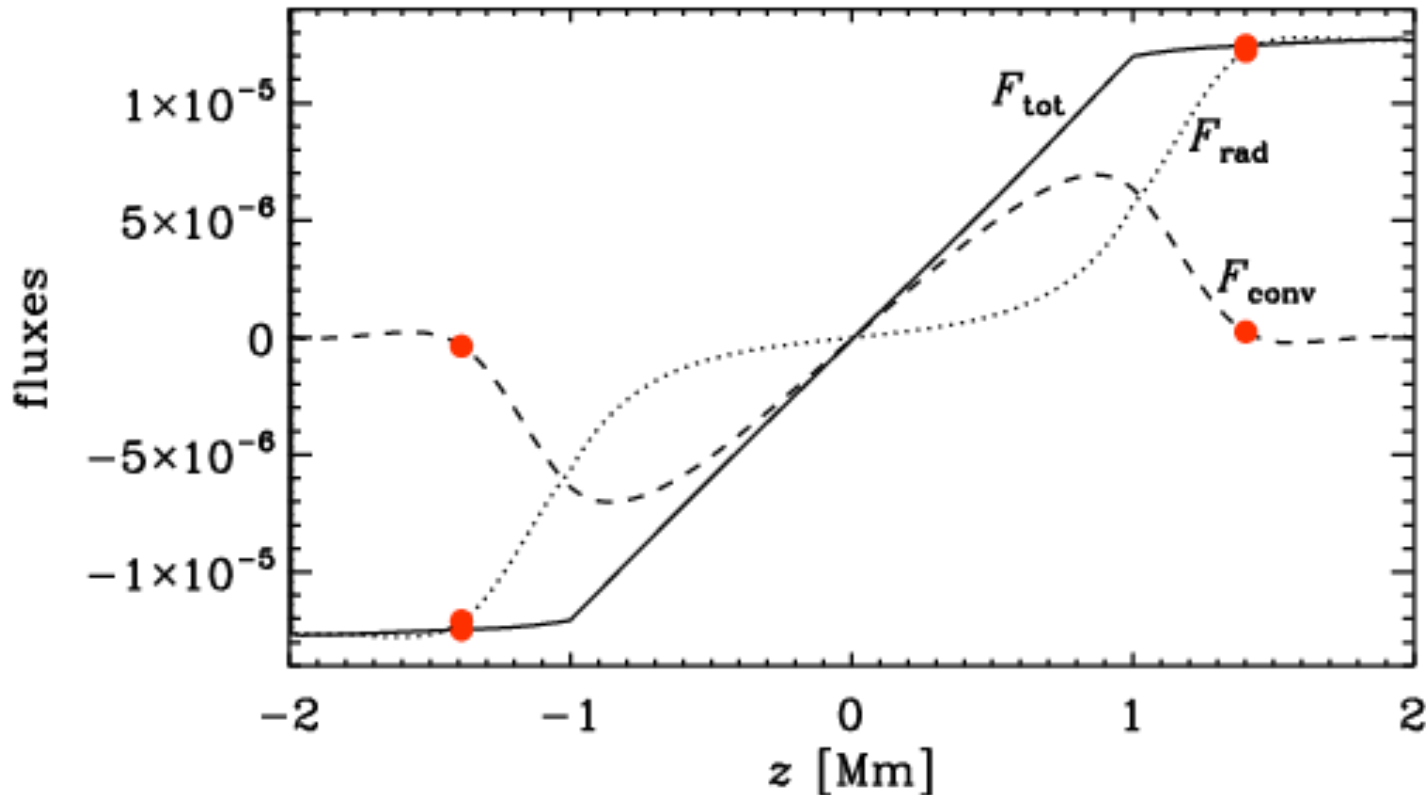
- Convection smears out negative entropy gradient
- Surface becomes slightly cooler

Strong random perturbations: almost die out



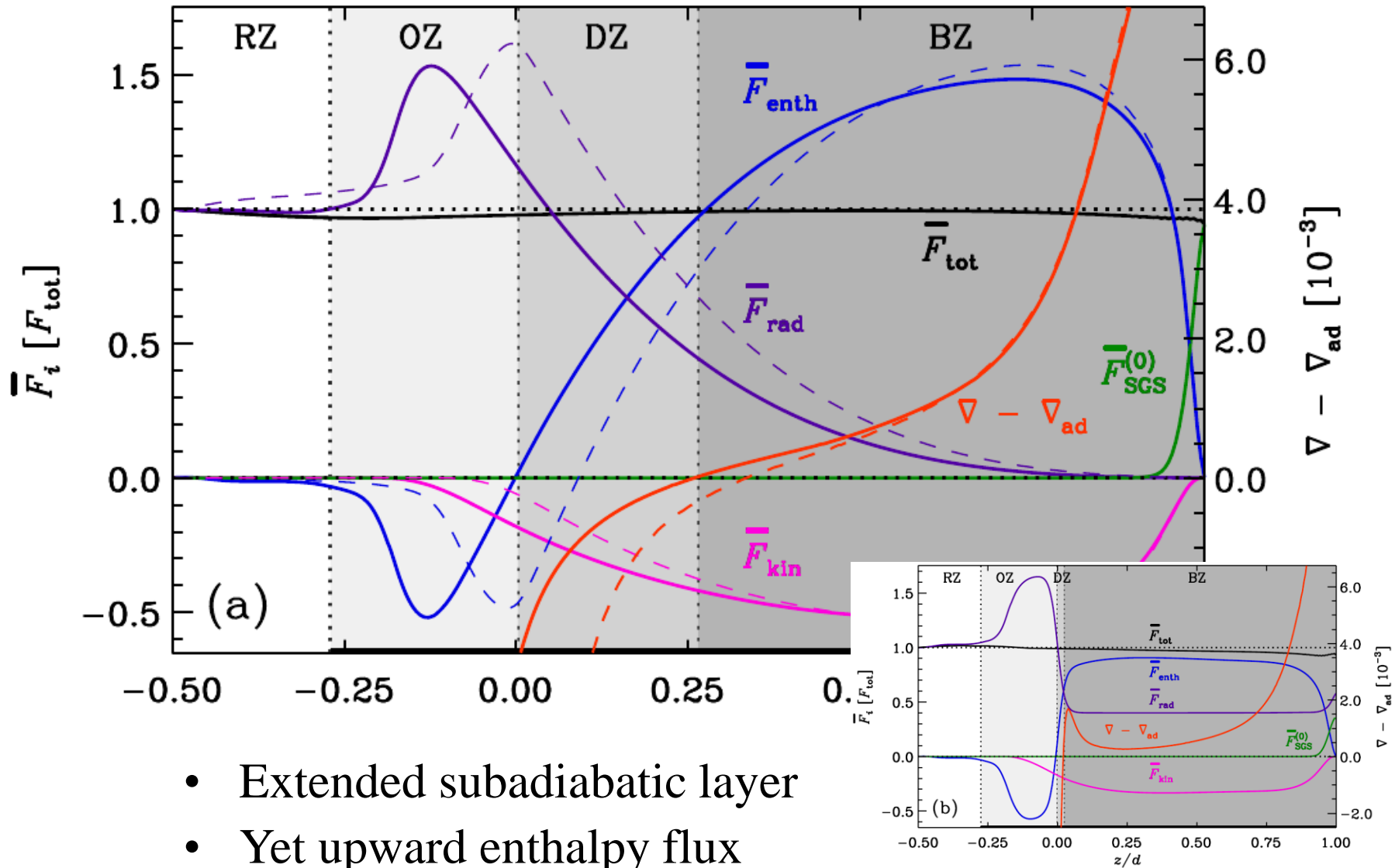
- Mild convection
- Strongly subsonic

Deardorff also in accretion discs



- Significant convective flux near midplane!
- Not explained by super-adiabatic gradient!

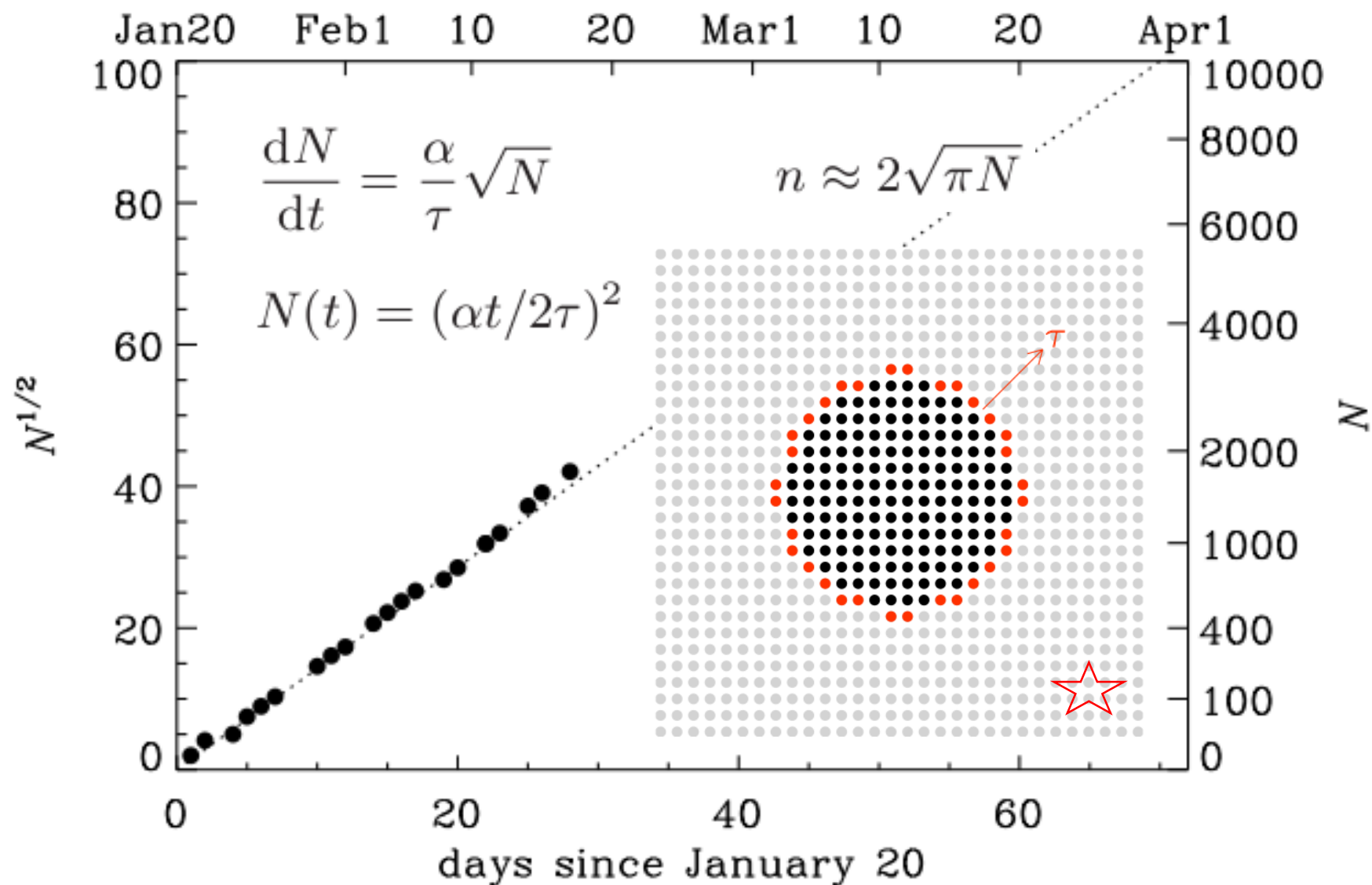
Simulations (Käpylä+17)



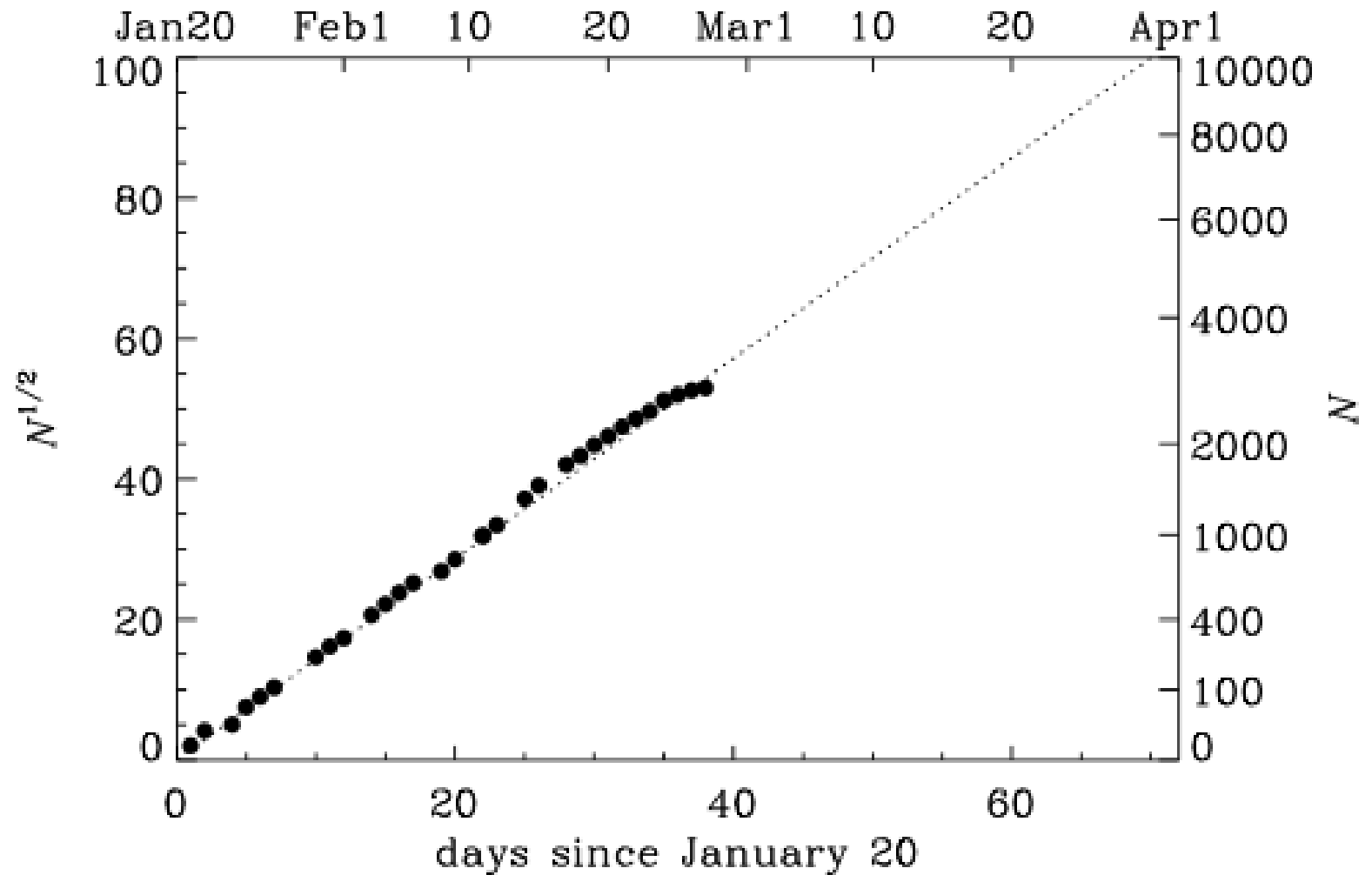
Consequences

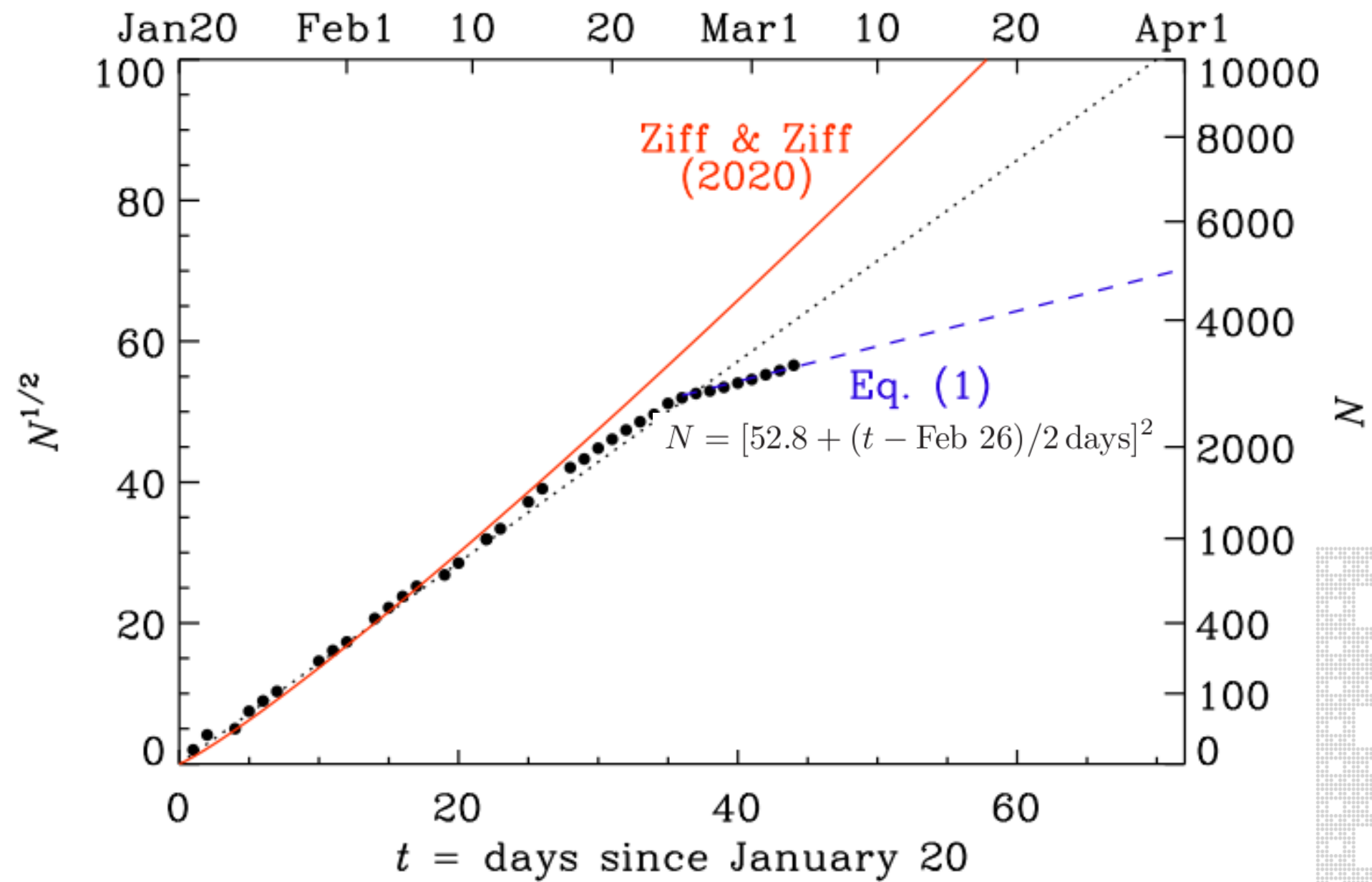
- Large scales not excited
 - No giant cell convection
- Smaller scale $l \rightarrow$ less turb. Diffusion: $\eta_t = lu_{\text{rms}}/3$
 - Applications to dynamos: stronger, less turb diffusive
- Two other important effect:
 - Lambda effect \rightarrow differential rotation
 - Negative effective magnetic pressure \rightarrow spots

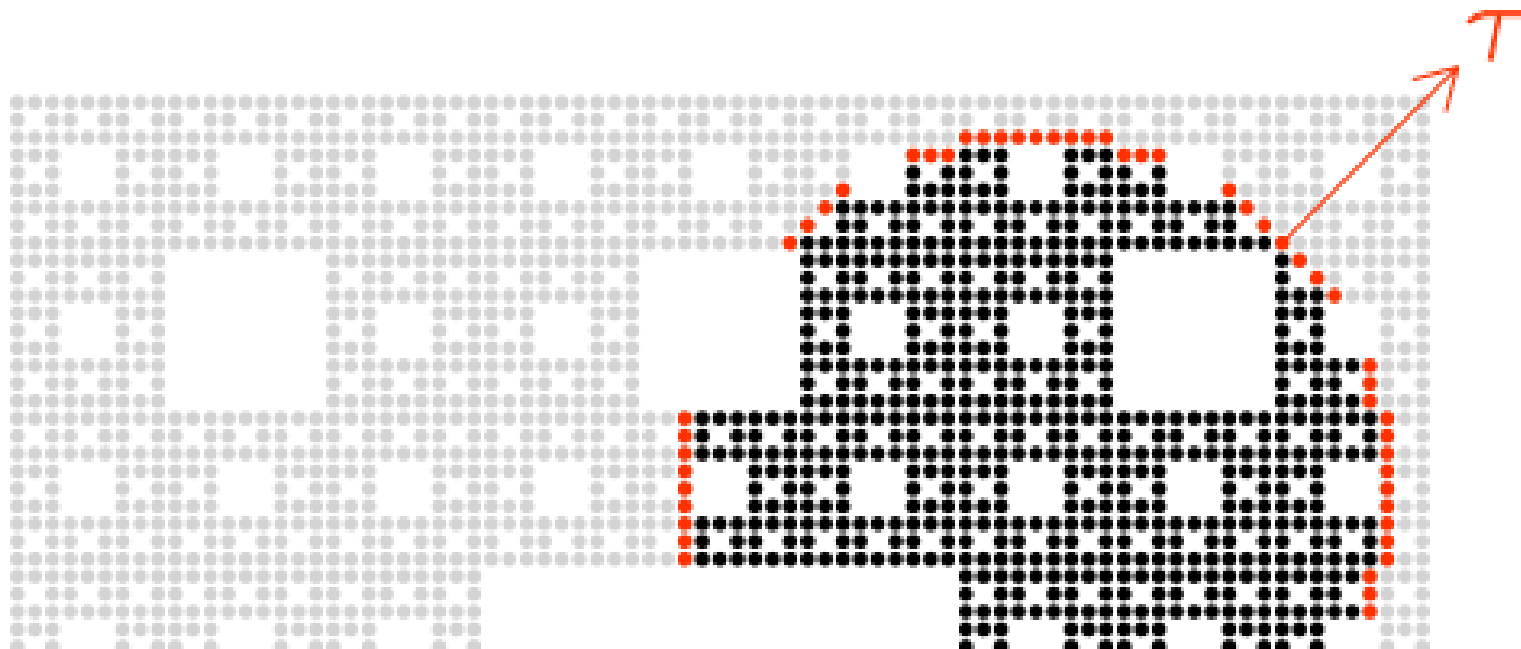
Coronaviral activity (update)



Latest update (last week)







Date and Time: Wednesday March 4, 15.15 - 16.15.

Location: Kräftriket House 5, Room 15.

Speaker: Tom Britton (SU)

Title: Mathematical modelling of infectious disease outbreaks

Abstract:

Mathematical models for the spread of infectious diseases are used to: better understand spreading mechanisms, determine if a big outbreak is likely to occur and how big it will be, determine if a disease will become endemic, and investigate how various preventive measures can reduce spreading hopefully preventing a major pandemic outbreak or make an endemic disease vanish. Making inference is harder than usual in that the basic events, transmissions, are rarely observed but instead proxies like onset of symptoms are recorded, and also by the fact that these events are dependent rather than independent (as is usually the case).

In the talk I will give an overview of the area with particular focus on emerging outbreaks, with illustrations on the current coronavirus outbreak.

<

○

Roslagstullsbacken 17

⋮

⬇

Matematiska institutionen, Stockh...

⬆

🚗 5 min

🚆 —

🚶 12 min

🚲 5 min

✈

12 min (900 m) Mostly flat.
via Albanovägen

Preview >>

⚠ Use caution—walking directions may not always reflect real-world conditions.

📍 Roslagstullsbacken 17
114 21 Stockholm

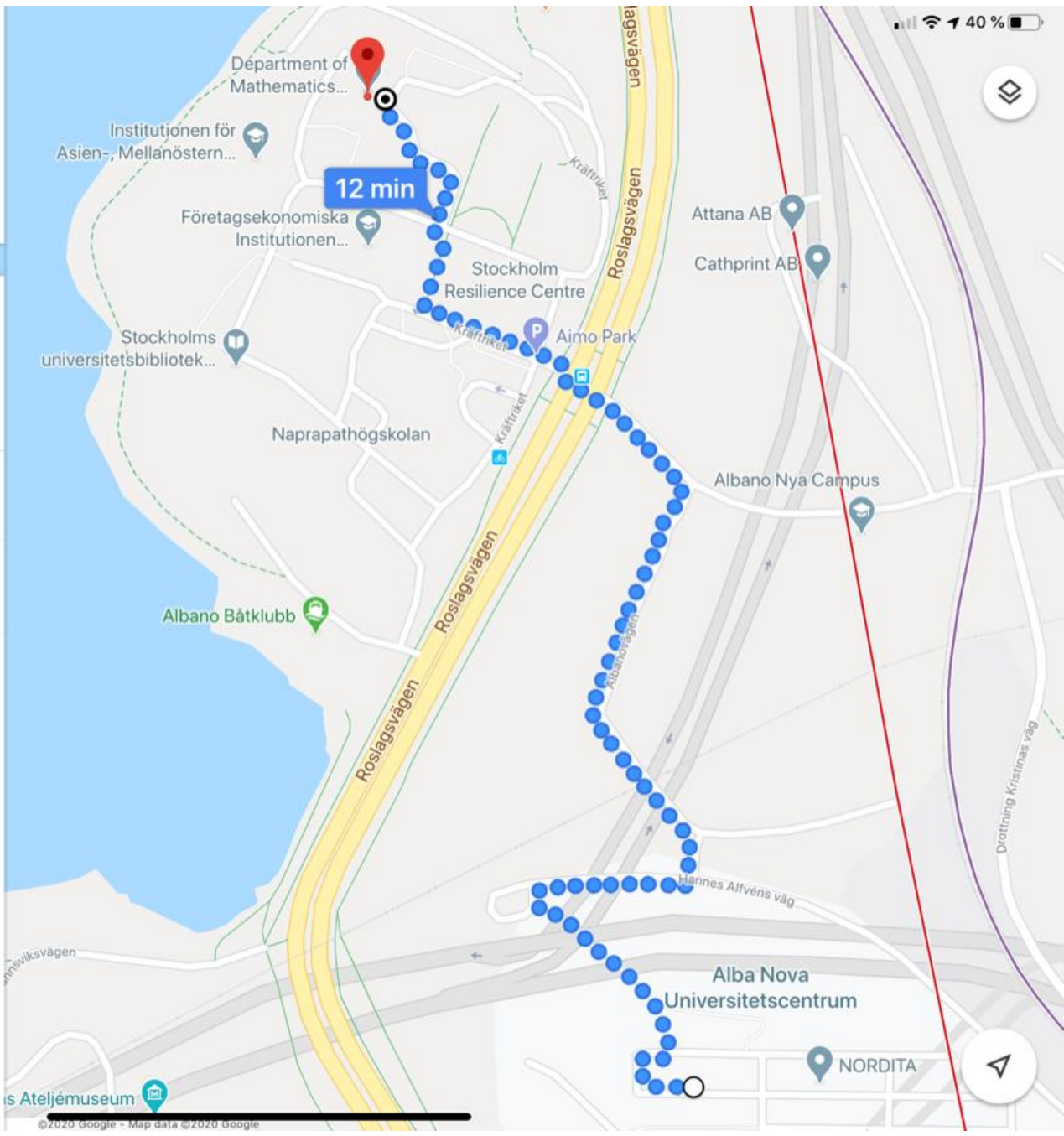
⬆ Head west on Roslagstullsbacken
80 metres

⬅ Turn left toward Hannes Alfvéns väg
Take the stairs
120 metres

➡ Turn right toward Hannes Alfvéns väg
10 metres

➡ Turn right onto Hannes Alfvéns väg
100 metres

⬅ Turn left toward Albanovägen
20 metres



Conclusions

- For the Sun: need new approaches
 - WholeSun (Paris, MPS, Oslo)
 - ERC consolitator for Maarit Käpylä
- Smart top boundary condition
 - Effects of entropy rain

Crafoord prize in Astronomy 2020



“for pioneering and fundamental studies of the solar wind and magnetic fields from stellar to galactic scales”